



The three-dimensional architecture of the human genome: understanding the physical mechanisms controlling gene expression



FAPESP School on Exact, Natural and Life Sciences
7-10 August 2022

José N. Onuchic
Center for Theoretical Biological Physics
CTBP
Rice University
ctbp.rice.edu



Peter Wolynes



Olga Dudchenko



Erez Aiden



Michele Di
Pierro



Ryan Cheng



Vinicius
Contessoto



Sumitabha
Brahmachari



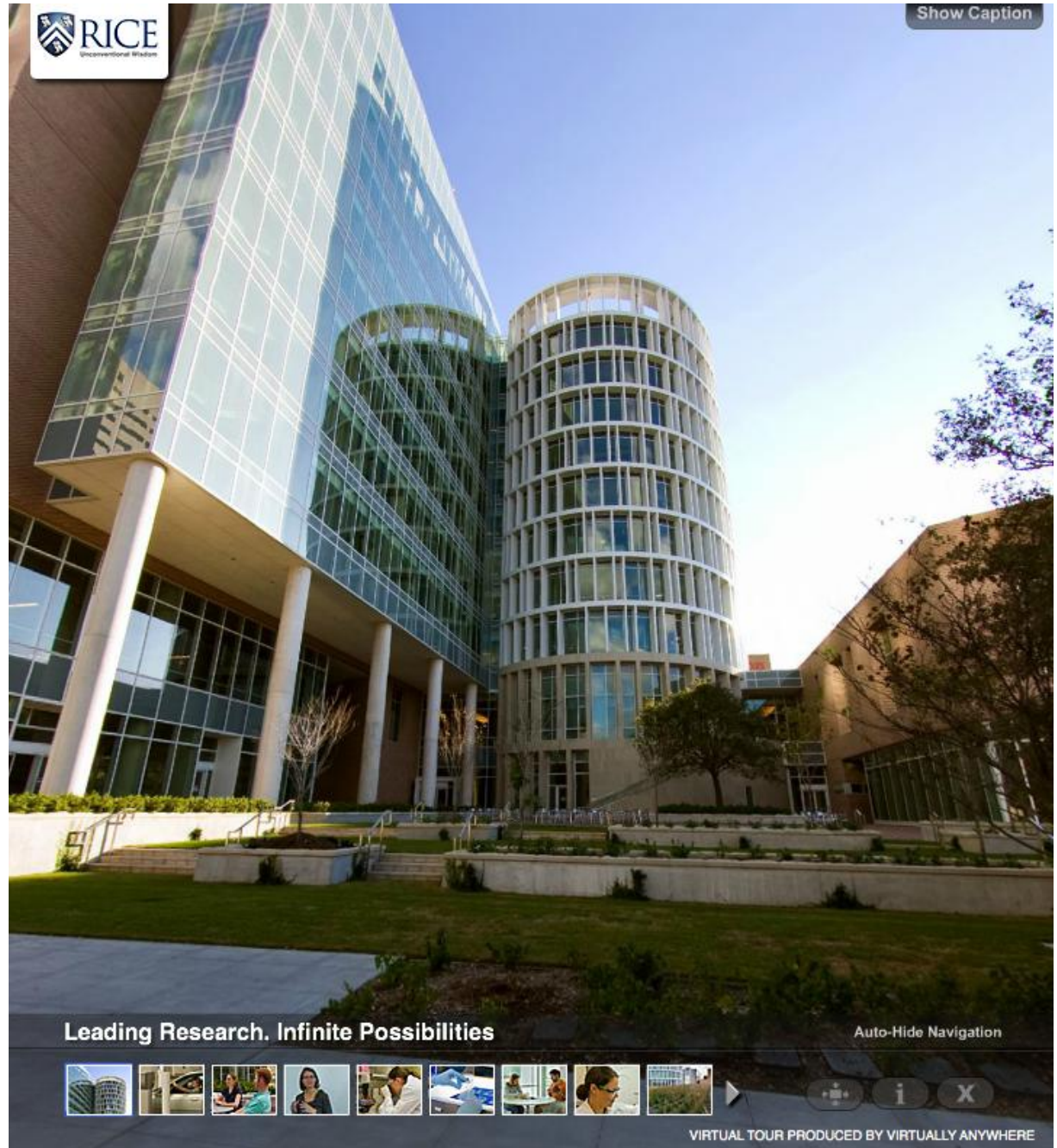
Antonio B.
De Oliveira Jr.





Center for Theoretical Biological Physics

10th floor of the BioScience Research Collaborative



Leading Research. Infinite Possibilities

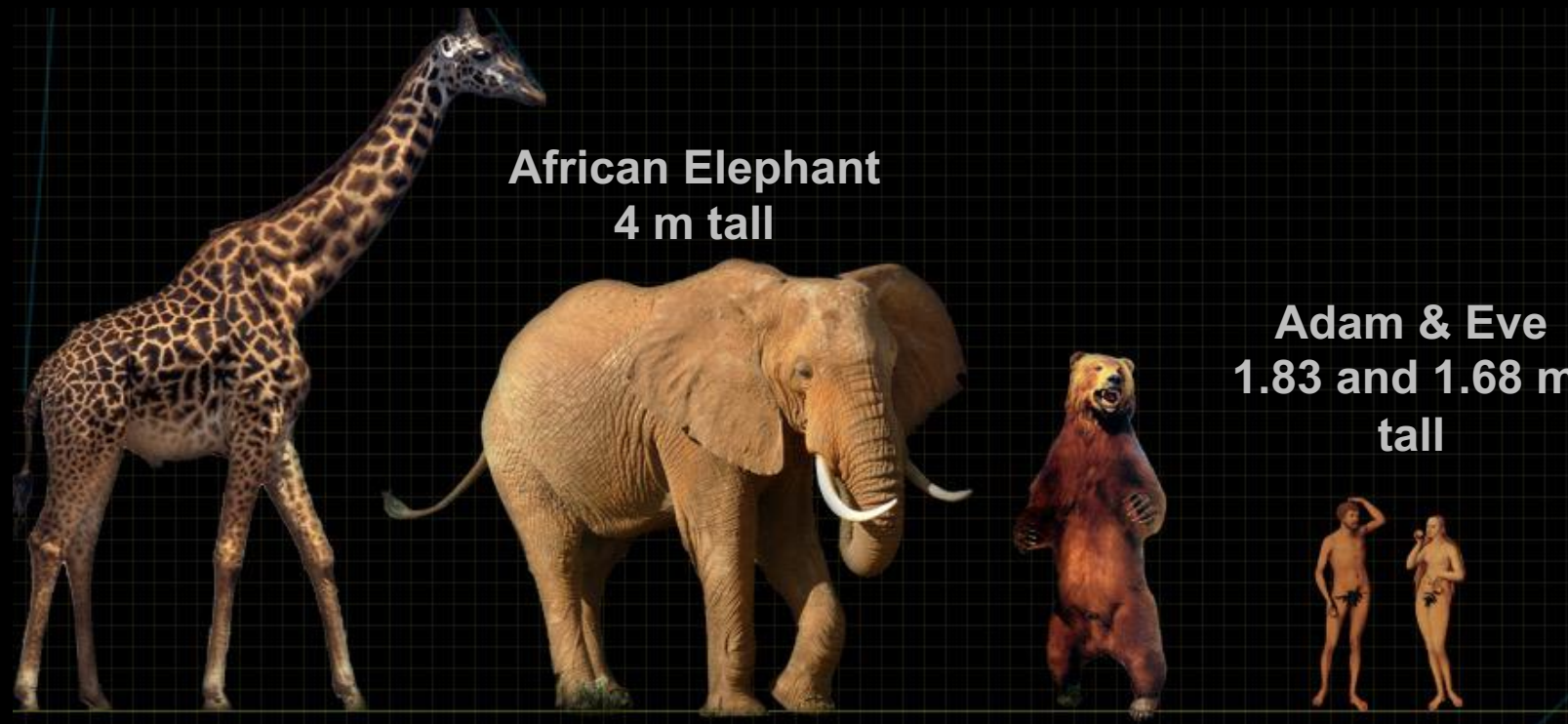
Auto-Hide Navigation



VIRTUAL TOUR PRODUCED BY VIRTUALLY ANYWHERE



Preface: A Short Survey of Length Scales

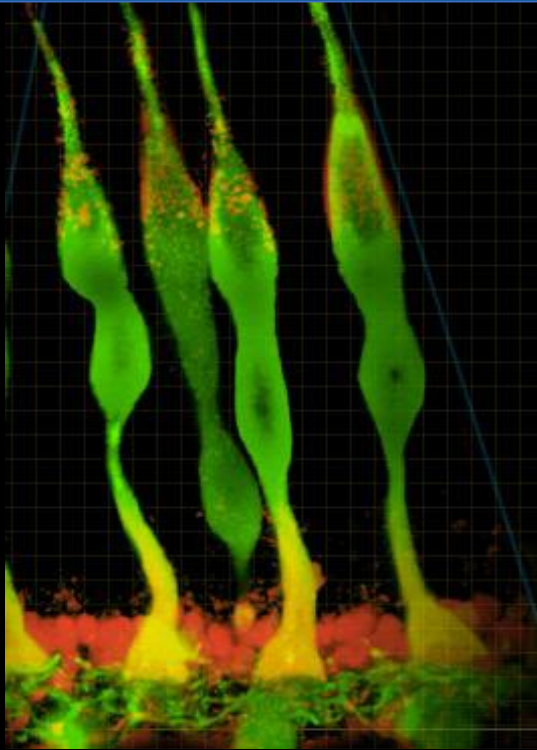


Giraffe
6.1 m tall

Kodiak
Bear 3 m
tall

**Our Genome
2 m long**

Preface: A Short Survey of Length Scales



Photoreceptors
 $1 \times 10^{-4} \text{ m}$



Sperm
 $6 \times 10^{-5} \text{ m}$

Cell Nucleus
 $6 \times 10^{-6} \text{ m}$



Metaphase
X Chromosome
 $7 \times 10^{-6} \text{ m}$



Yeast
 $3 \times 10^{-6} \text{ m}$

DNA must be open and knots free

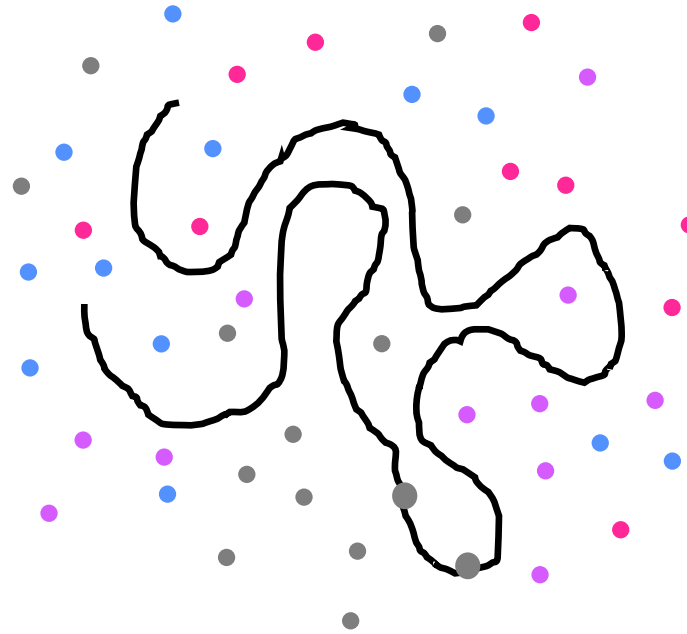


Very little accessible tape!

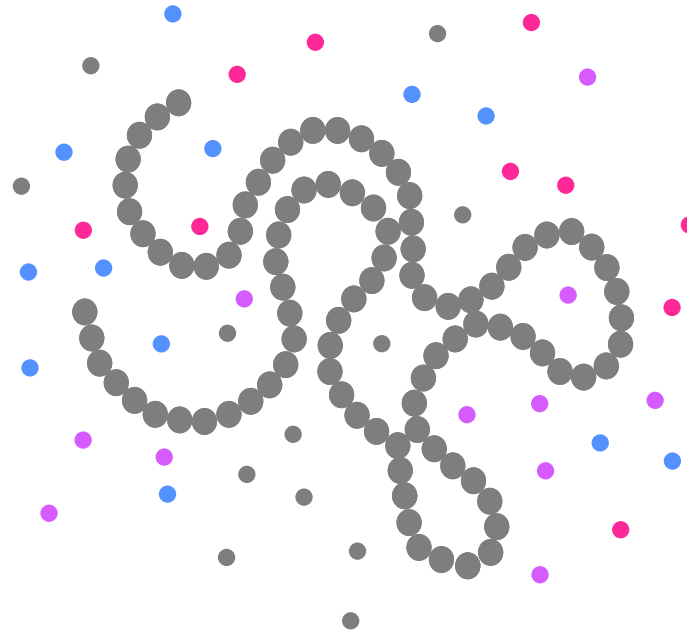


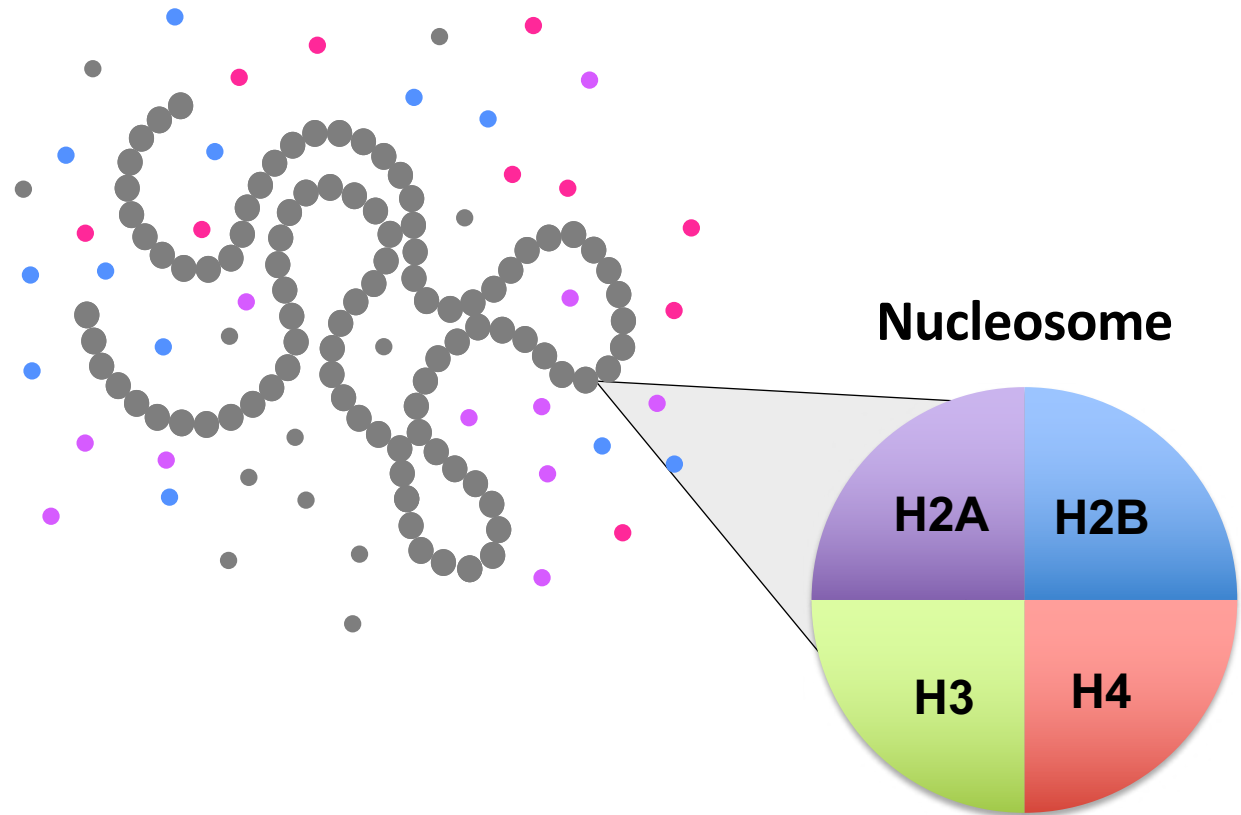
Knots don't help reading!

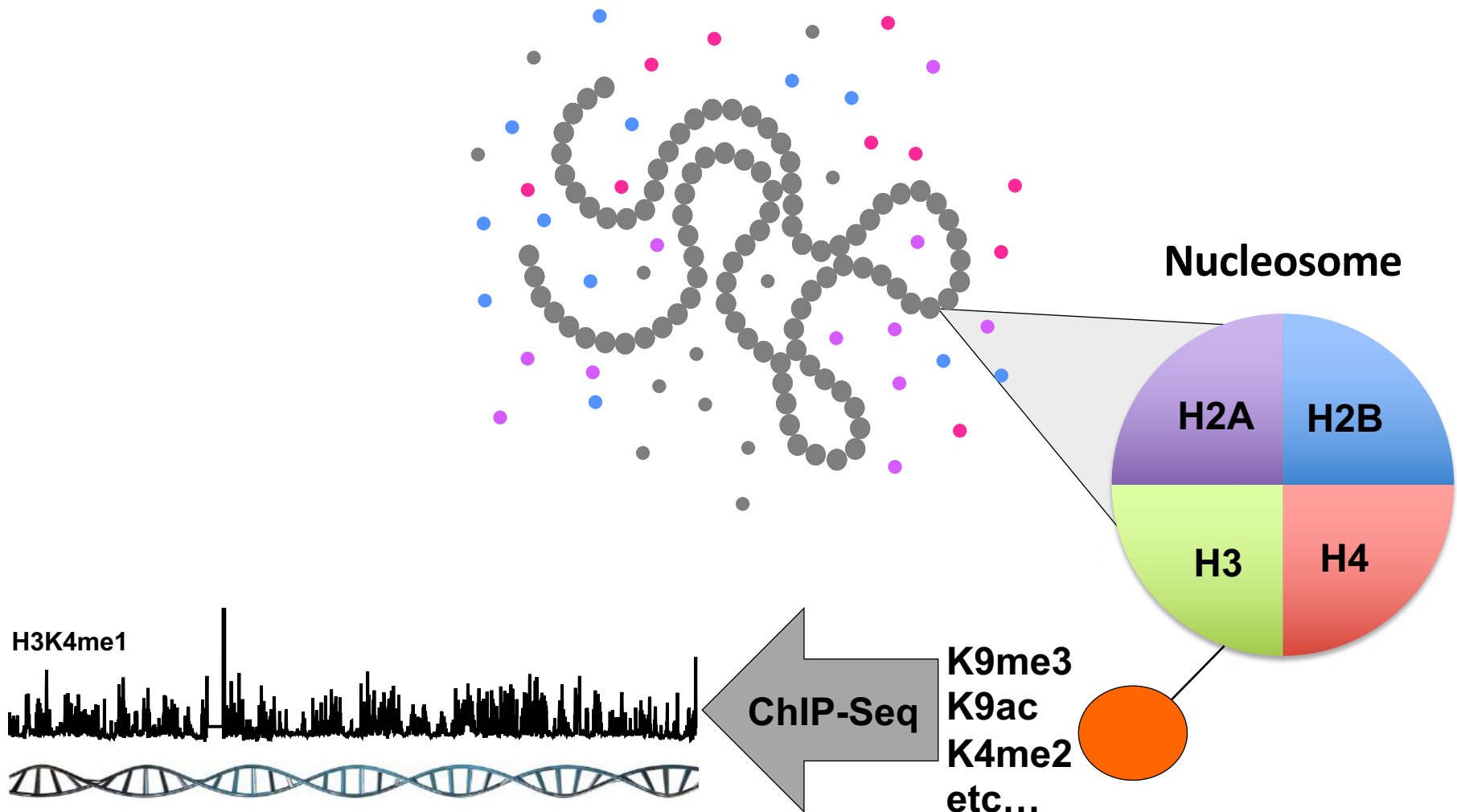




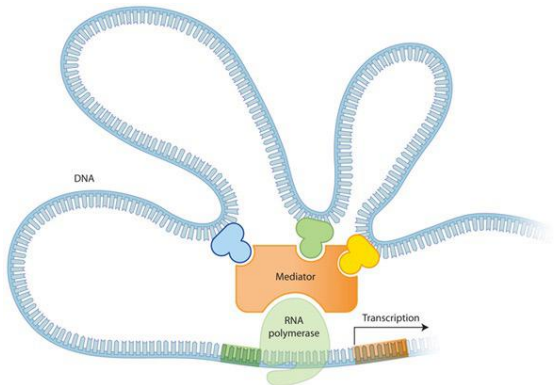
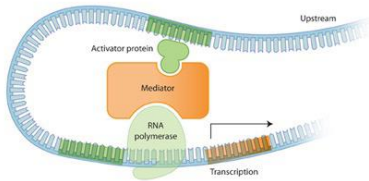
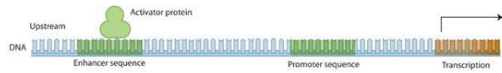
A Complex Polymer In A Complex Environment





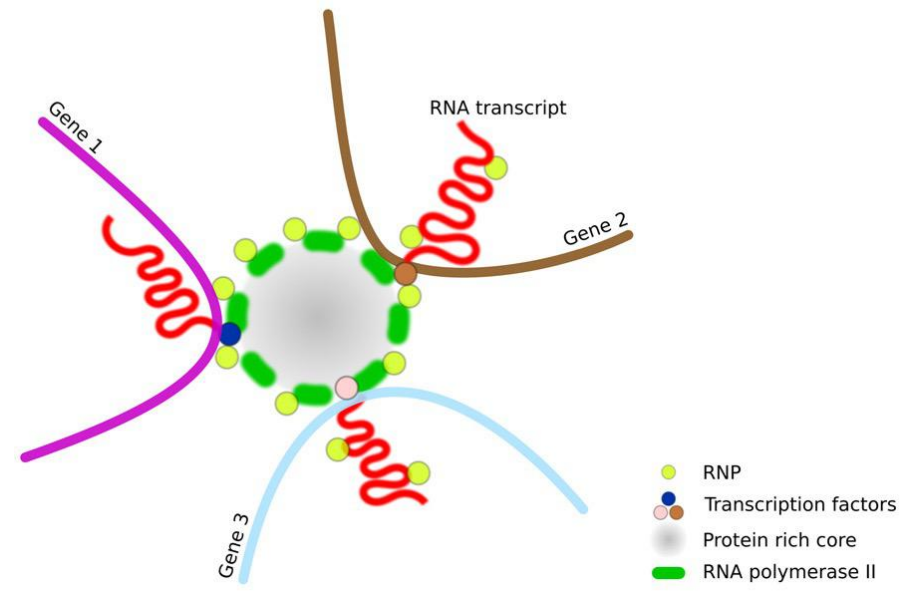


Enhancers



Transcription Factories

Structure of a transcription factory



© Nature Education

Rieder *et al.* 2012

**Fluorescence *In Situ*
Hybridization (FISH)**

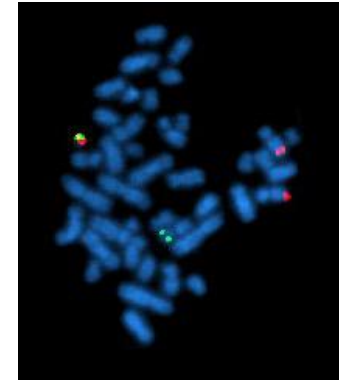
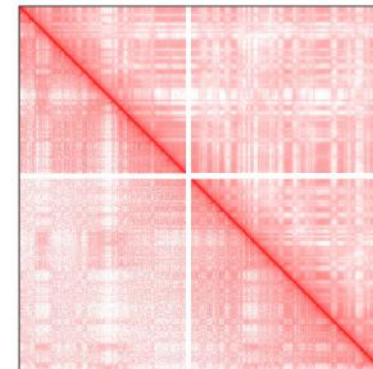
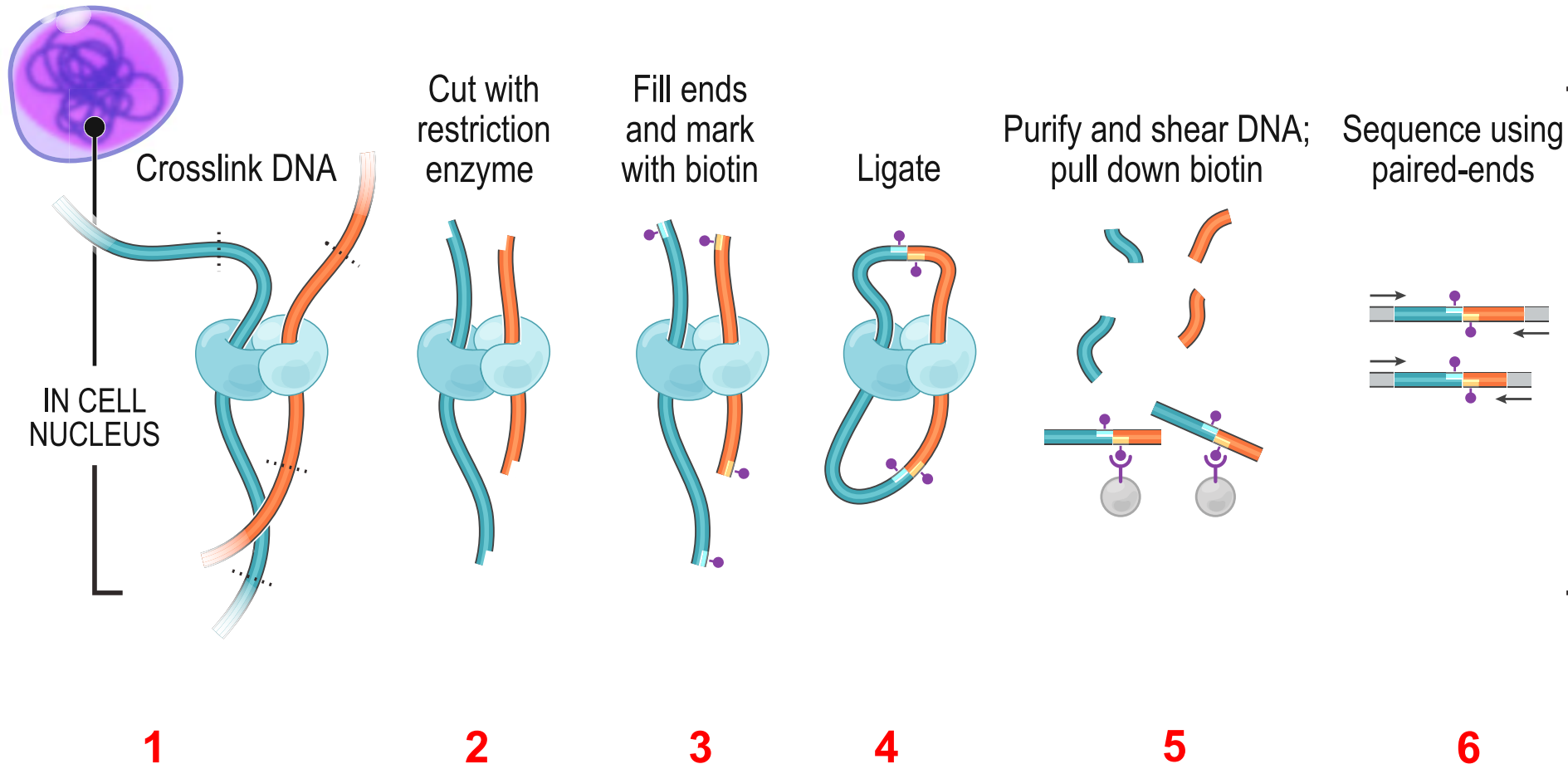


Image from Wikipedia

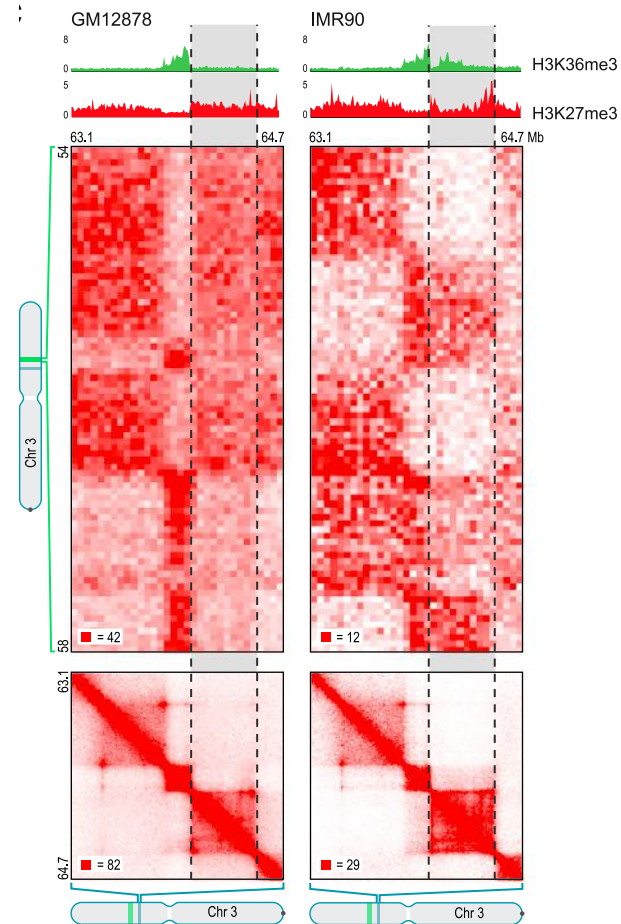
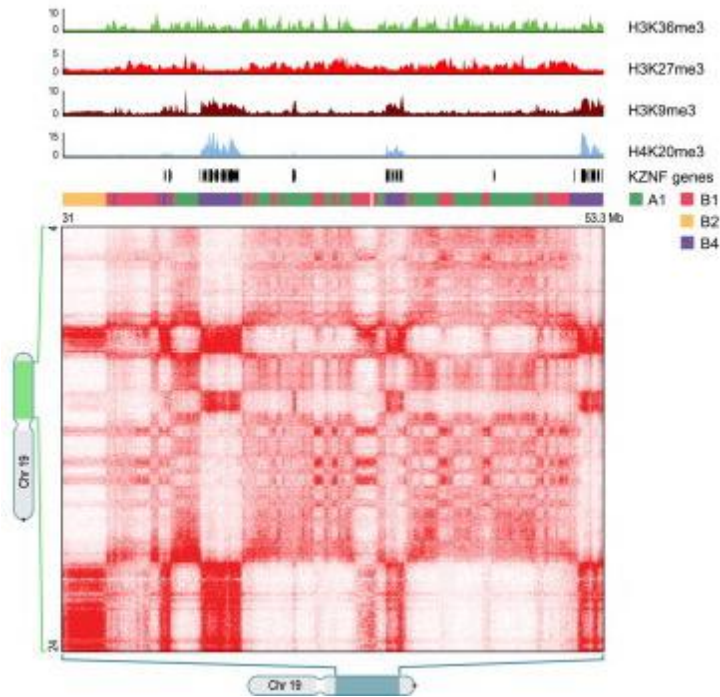
**Chromosome
Conformation Capture
(3C, 4C, 5C, Hi-C)**





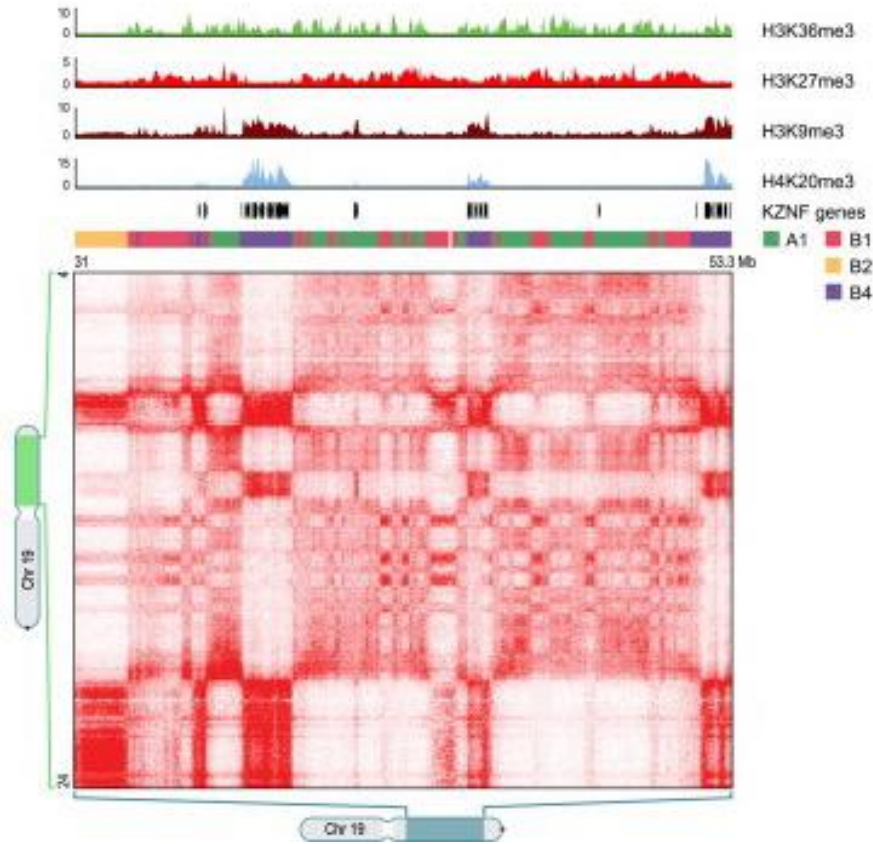
Rao *et al.* 2014

Chromatin Architecture is Specific to the Cell Type

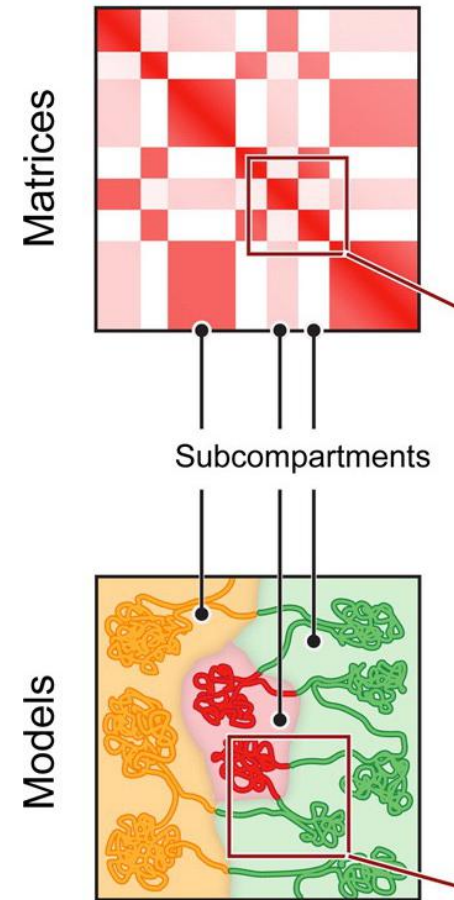


Lieberman Aiden Lab

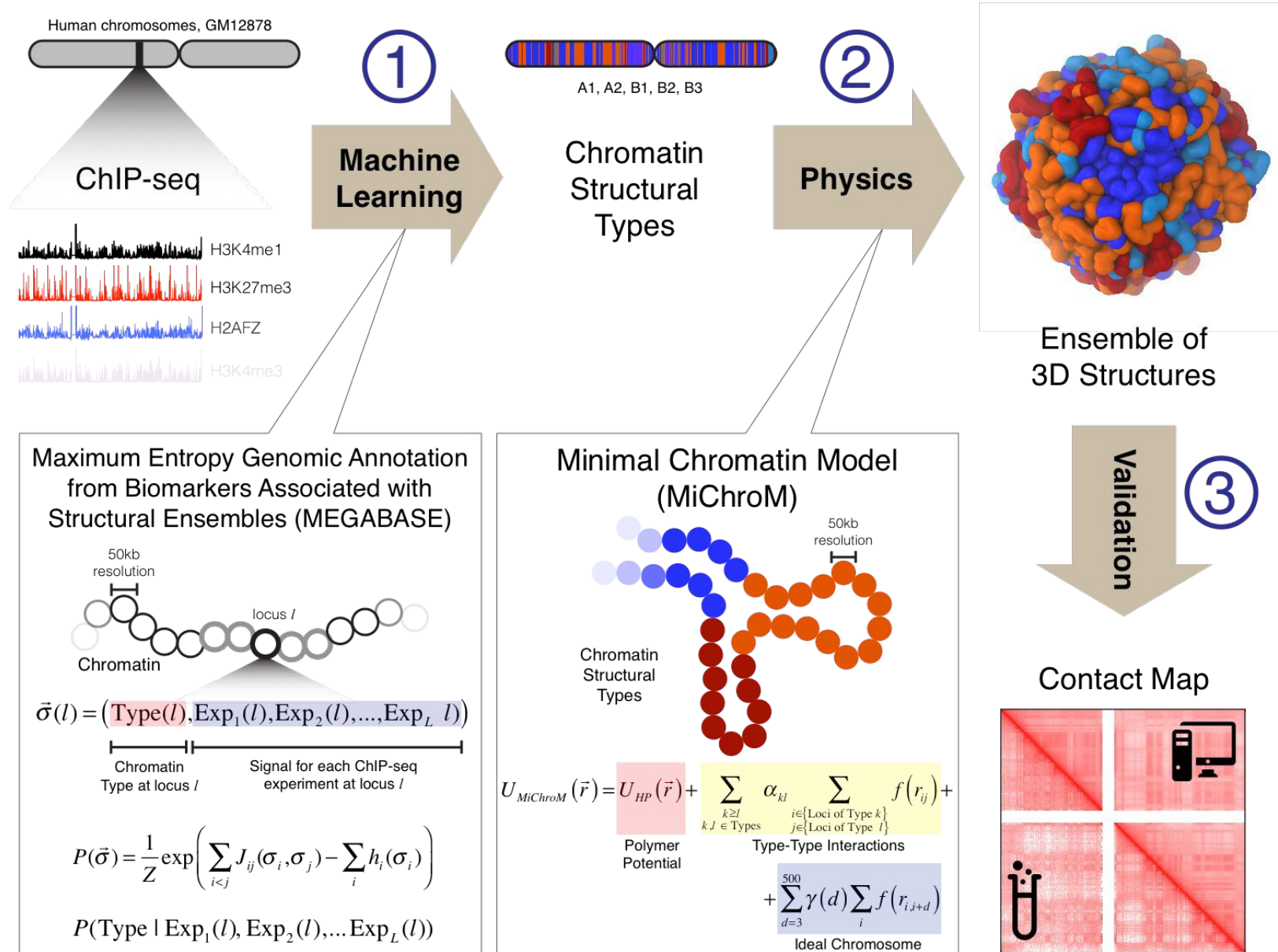
DNA-DNA Ligation Experiments Reveals Compartments which appear to correlate with epigenetic modifications



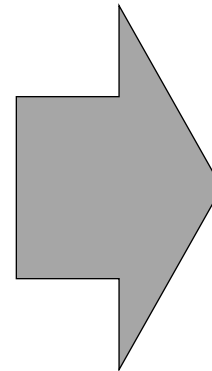
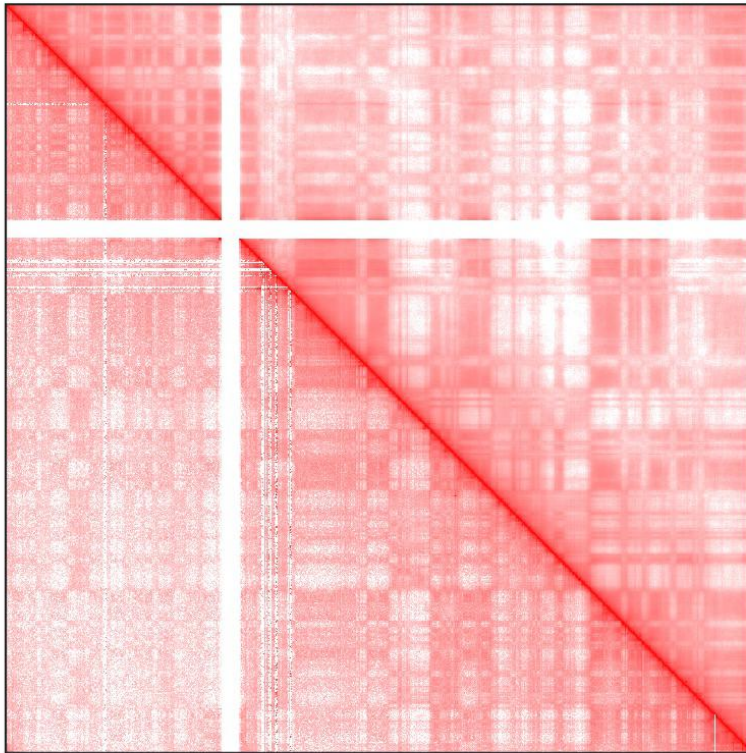
Patterns in contact probabilities identify 6 chromatin types (Sub-compartments):
A1, A2, B1, B2, B3, B4



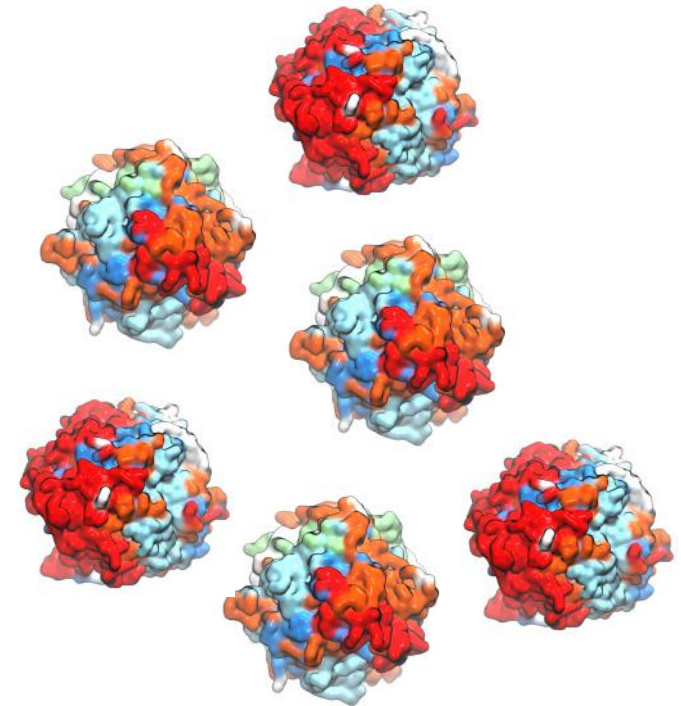
Schematic Illustration of Computational Pipeline



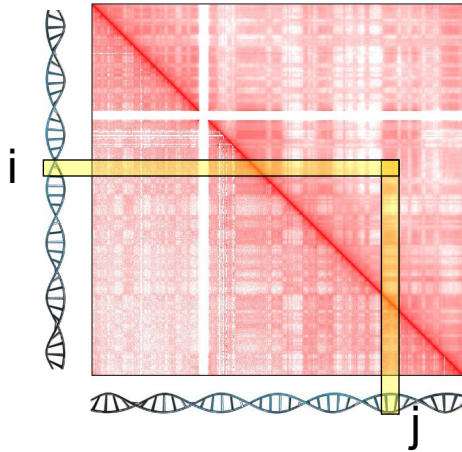
DNA-DNA ligation Assays: Hi-C



Structural Ensemble



1 Chromosome, 1 Conformation, 1 Experiment

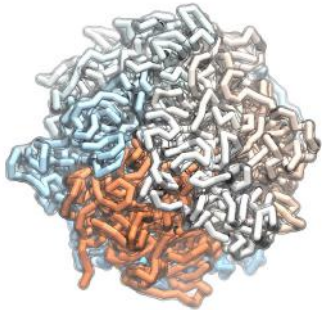


Did *i* and *j* crosslink?

- yes/no

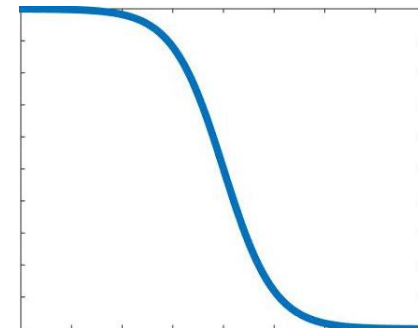
How often did *i* and *j* crosslink?

- A lot when they are close, not much when they are far.



$$f_{ij} = f(r_{ij})$$

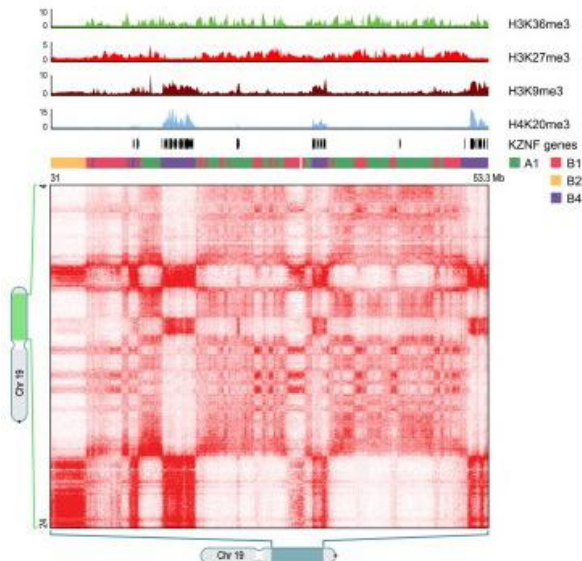
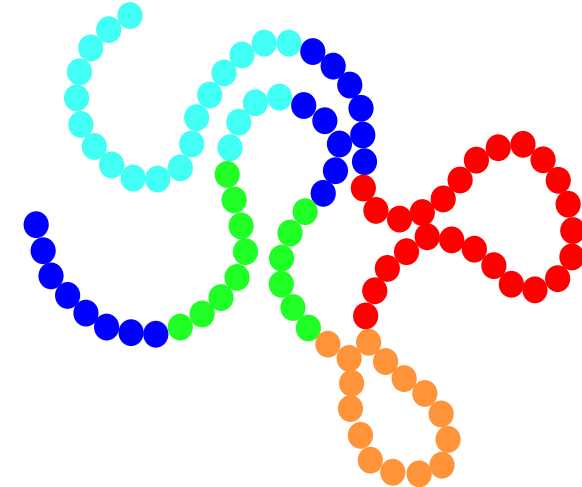
$$p_{ij} = \langle f(r_{ij}) \rangle$$



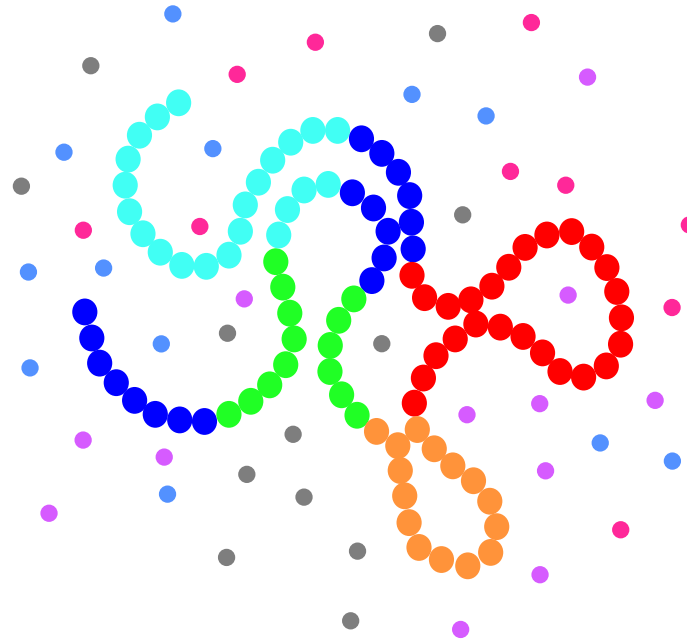
The Minimal Chromatin Model (MiChroM): Phase Separation

Fact 1. Phase Separation of Chromatin Structural Types

If and when two segments of chromatin form a contact the energy of the contact depends only on the type identity of the contact.



The Minimal Chromatin Model: Some Motivated Physical Assumptions



Implicit Protein Model

Type-to-Type Interactions are mediated by a cloud of proteins that bind with different selectivity to different sections of chromatin

The Minimal Chromatin Model: Some Motivated Physical Assumptions

Fact #2:

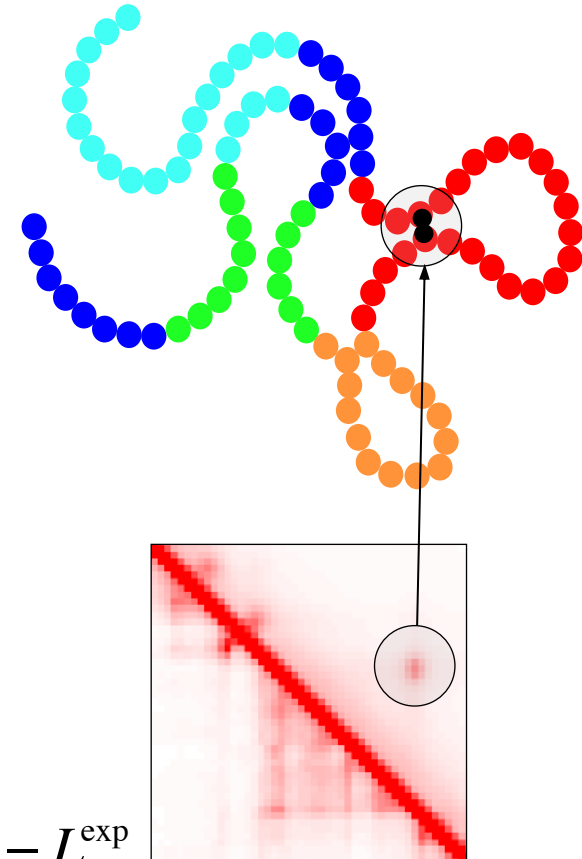
Chromatin form loops at specific locations related to the activity of the protein CTCF

Phillips and Corces 2009

Rao *et al.* 2014

Physical Assumption #2:

If and when the two ends of a loop come into contact, an there is an additional gain in effective free energy



Observable

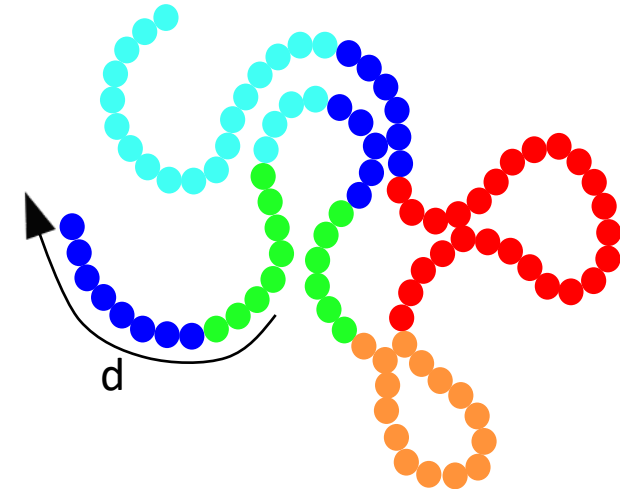
$$L(\vec{r}) = \sum_{(i,j) \in \{\text{Loops Sites}\}} f(r_{ij})$$

Constraint

$$c_L = \int L(\vec{r}) \pi^{\text{MiChroM}}(\vec{r}) d\vec{r} - L^{\text{exp}}$$

Fact #3: The effect of all protein motors acting along the DNA polymer

Ideal Chromosome/Lengthwise Compaction.
Every time two loci at genomic distance d come into contact there is a gain/loss of $\gamma(d)$ effective free energy.



A translational invariant function of the genomic distance consistent with

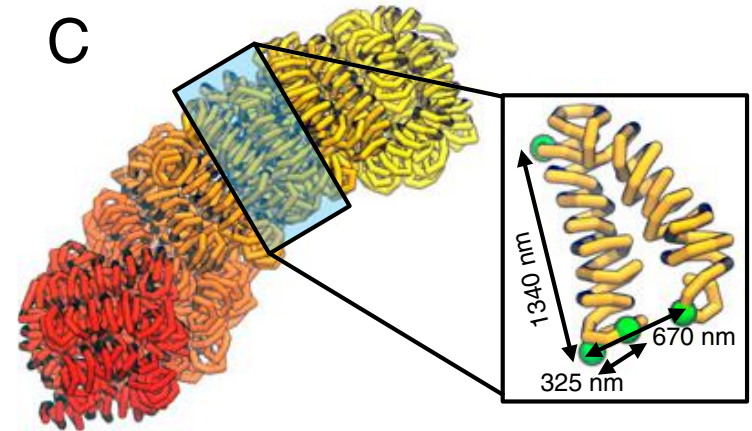
- the notion of a higher order fiber in chromatin
- liquid crystal behavior

But more general...

M.D.P. , B. Zhang, E. Lieberman Aiden, P. G. Wolynes, and J. N. Onuchic, *PNAS* 2016
B. Zhang and P. G. Wolynes, *PNAS* 2015

- **A translational invariant function of the genomic distance**
- **Consistent with**
 - the notion of a higher order fiber in chromatin
 - liquid crystal behavior

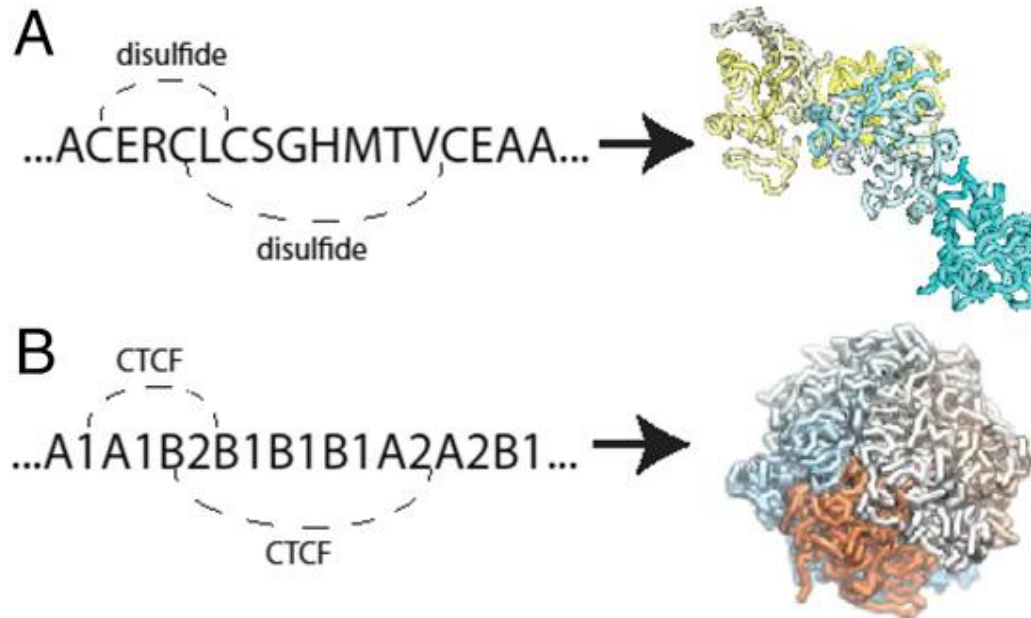
But more general...



Zhang and Wolynes 2015

The Minimal Chromatin Model (MiChroM): Phase Separation

A one-dimensional sequence encodes the three-dimensional fold of chromosomes



with



Bin Zhang

M.D.P. , B. Zhang, E. Lieberman Aiden, P. G. Wolynes, and J. N. Onuchic, *PNAS* 2016
+ Commentary by G. Gürsoy and J. Liang, *PNAS* 2016

The Minimal Chromatin Model: 3 Simple Physical Assumptions

Physical Assumption

Observable

Constraint

#1 If and when two segments of chromatin form a contact the energy of the contact depends only on the type identity of the contact.

Rao et al., 2014, Fillion et al., 2010

$$T_{kl}(\vec{r}) = \sum_{\substack{i \in \{\text{Loci of Type } k\} \\ j \in \{\text{Loci of Type } l\}}} f(r_{ij})$$

$$c_T^{kl} = \int T_{kl}(\vec{r}) \pi^{\text{MiChroM}}(\vec{r}) d\vec{r} - T_{kl}^{\text{exp}}$$

#2 If and when the two anchors of a CTCF-mediated loop come into contact, there is an additional gain in effective free energy

Phillips and Corces, 2009, Rao et al., 2014

$$L(\vec{r}) = \sum_{(i,j) \in \{\text{Loops Sites}\}} f(r_{ij})$$

$$c_L = \int L(\vec{r}) \pi^{\text{MiChroM}}(\vec{r}) d\vec{r} - L^{\text{exp}}$$

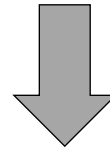
#3 Ideal Chromosome/Local Compaction. Every time two loci at genomic distance d come into contact there is a gain/loss of $\gamma(d)$ effective free energy.

$$G_d(\vec{r}) = \sum_i f(r_{i,i+d})$$

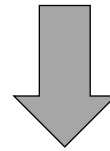
$$c_G^d = \int G_d(\vec{r}) \pi^{\text{MiChroM}}(\vec{r}) d\vec{r} - G_d^{\text{exp}}$$

The Minimal Chromatin Model (MiChroM): the Effective Energy Function

Constraints



Maximum Entropy Principle



Information Theoretic Energy Function

$$U_{MiChroM}(\vec{r}) = U_{HP}(\vec{r}) + \sum_{\substack{k \geq l \\ k, l \in \text{Types}}} \alpha_{kl} \sum_{\substack{i \in \{\text{Loci of Type } k\} \\ j \in \{\text{Loci of Type } l\}}} f(r_{ij}) + \chi \cdot \sum_{(i,j) \in \{\text{Loop Sites}\}} f(r_{ij}) + \sum_{d=3}^{500} \gamma(d) \sum_i f(r_{i,i+d})$$

Polymer
Potential

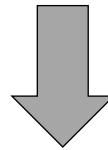
Type-to-Type
Interactions

Specific
Interactions

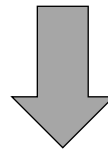
Lengthwise
Compaction

M.D.P. , B. Zhang, E. Lieberman Aiden, P. G. Wolynes, and J. N. Onuchic, *PNAS* 2016
+ Commentary by G. Gürsoy and J. Liang, *PNAS* 2016

Constraints



Maximum Entropy Principle



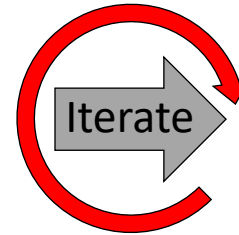
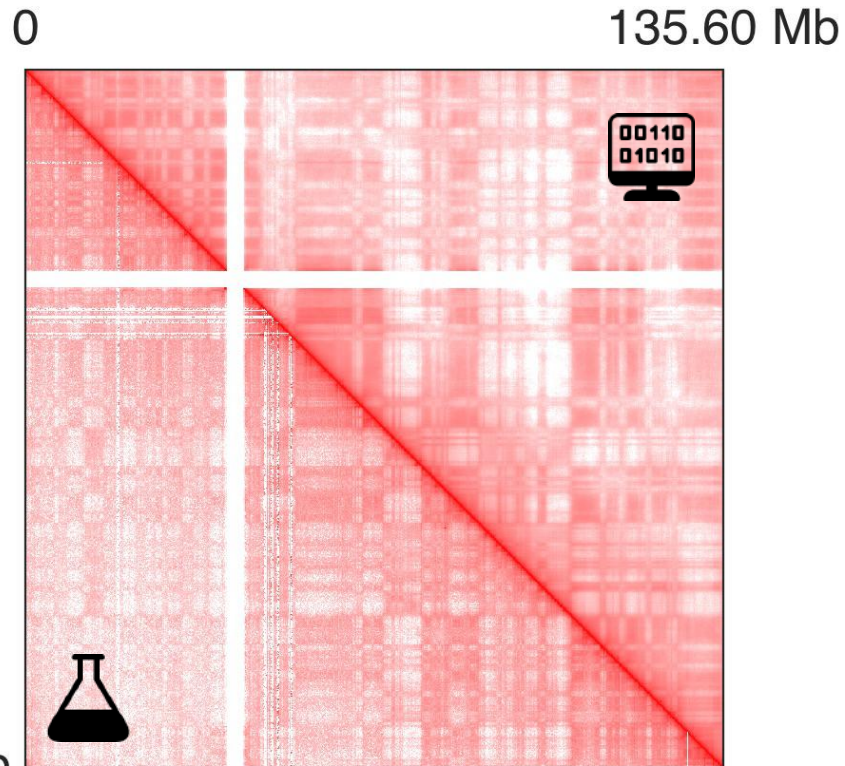
Information Theoretic Energy Function

$$U_{MiChroM}(\vec{r}) = U_{HP}(\vec{r}) + \sum_{\substack{k \geq l \\ k, l \in \text{Types}}} \alpha_{kl} \sum_{\substack{i \in \{\text{Loci of Type } k\} \\ j \in \{\text{Loci of Type } l\}}} f(r_{ij}) + \chi \cdot \sum_{(i,j) \in \{\text{Loop Sites}\}} f(r_{ij}) + \sum_{d=3}^{500} \gamma(d) \sum_i f(r_{i,i+d})$$

To Be
Determined...

The Minimal Chromatin Model: Calibration

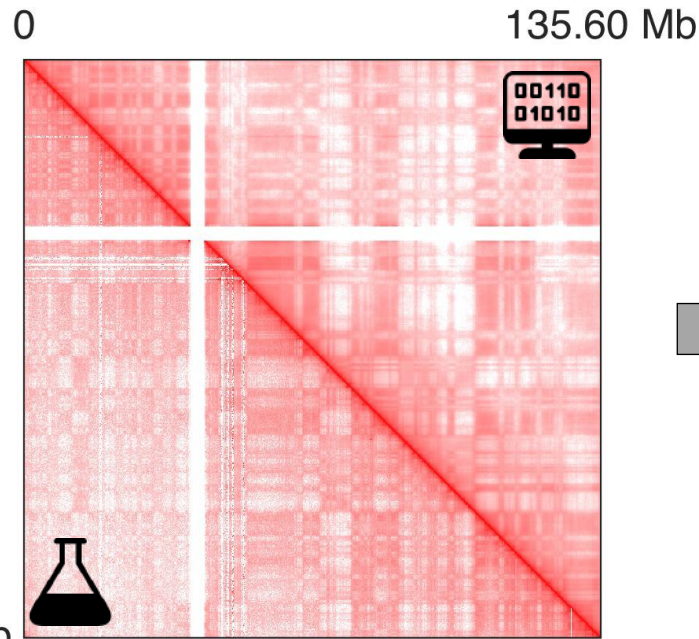
Human Chromosome 10 B-lymphoblastoid cells (GM12878)



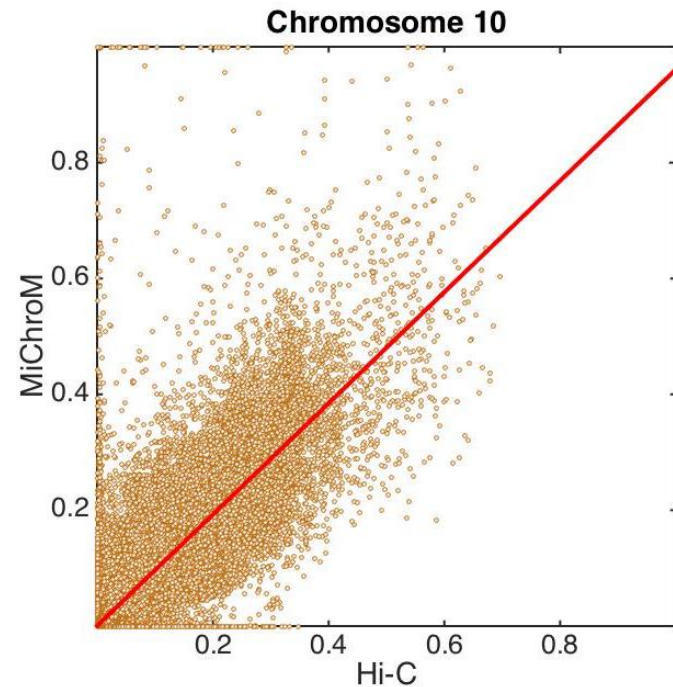
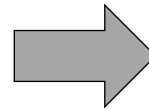
$$(\alpha_{kl}, \gamma(d), \chi)$$

The Minimal Chromatin Model: Quality Check

Human Chromosome 10 B-lymphoblastoid cells (GM12878)

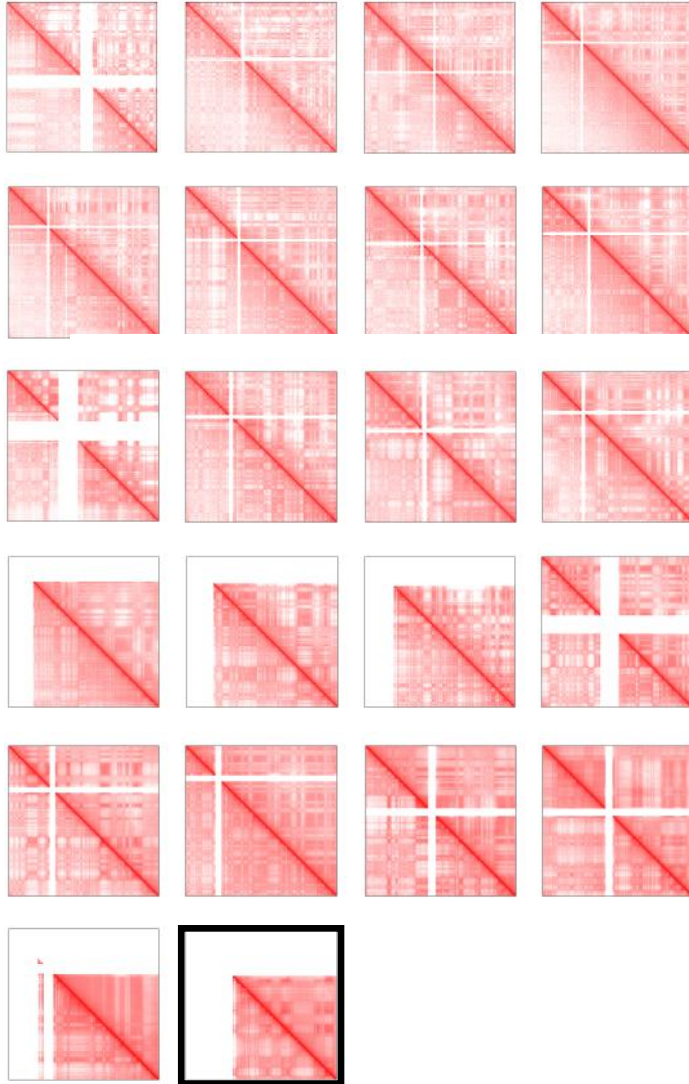


Pearson's Correlation 0.95



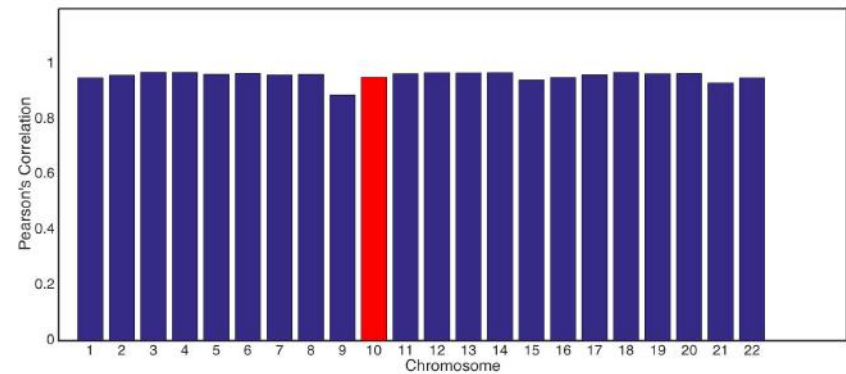
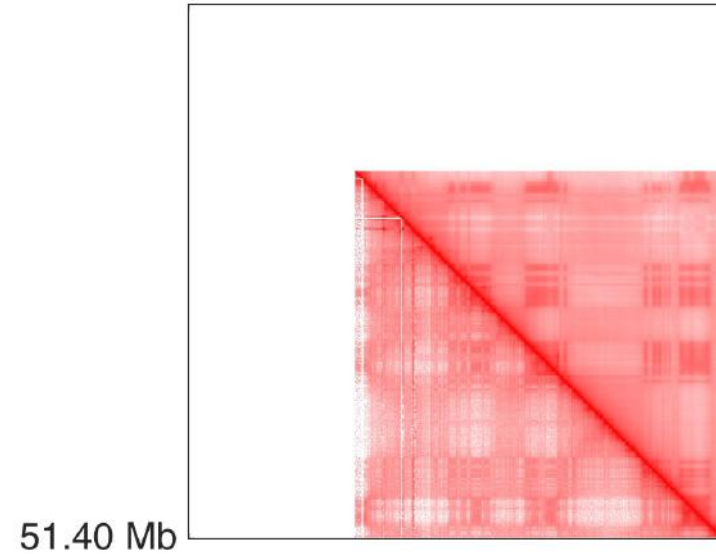
Slope 0.94
Intercept 0.0003

The Minimal Chromatin Model: Predictivity



Chromosome 22 (GM12878)

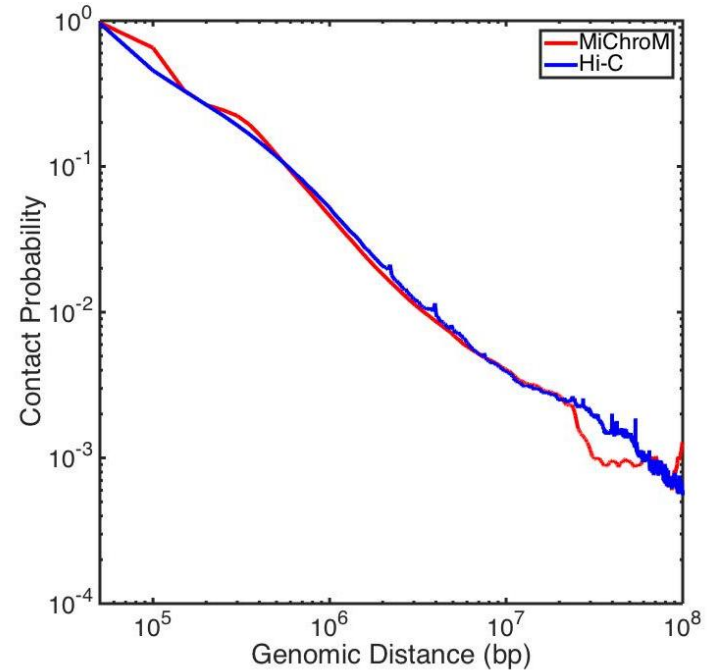
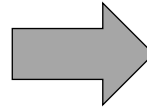
0 51.40 Mb



The Minimal Chromatin Model: Quality Check

Human Chromosome 10 B-lymphoblastoid cells (GM12878)

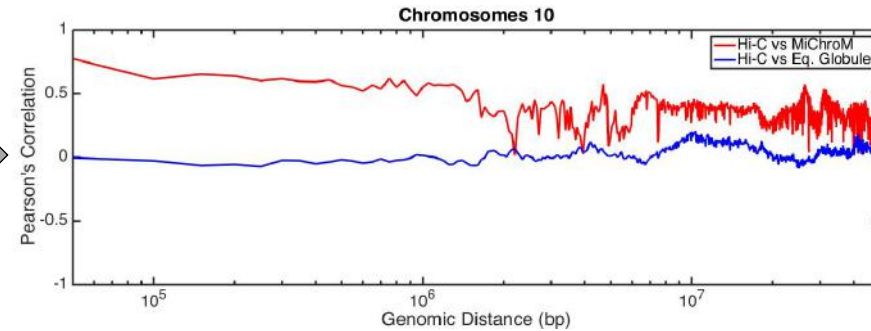
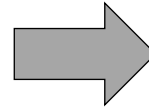
0 135.60 Mb



The Minimal Chromatin Model: Quality Check

Human Chromosome 10 B-lymphoblastoid cells (GM12878)

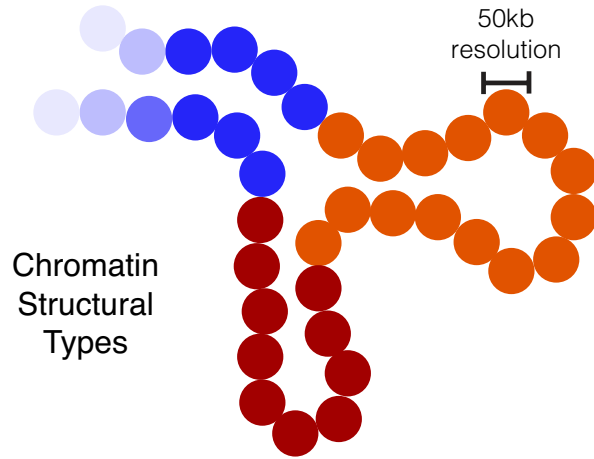
0 135.60 Mb



135.60 Mb

A physical polymer model with discrete chromatin types captures compartmentalization

Minimal Chromatin Model (MiChroM)

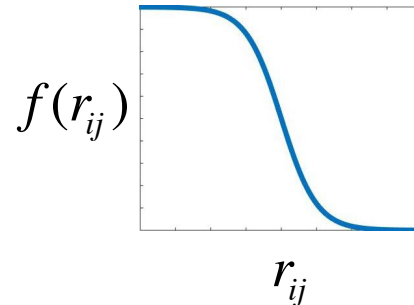
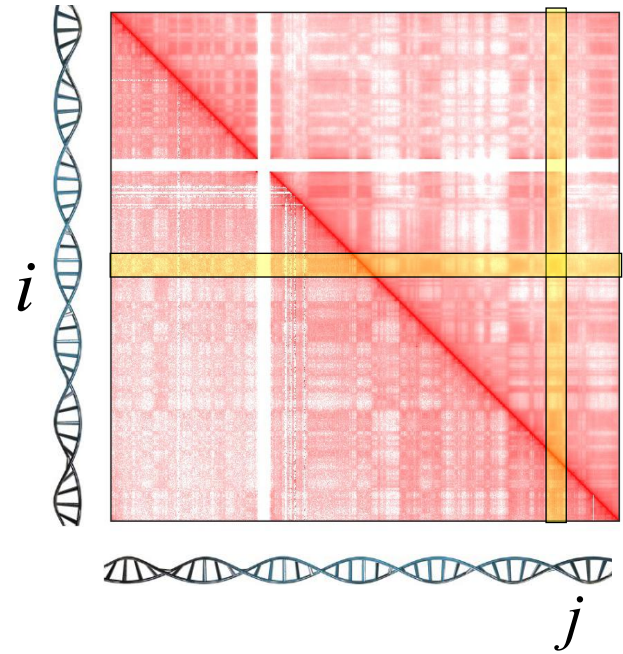


$$U_{MiChroM}(\vec{r}) = U_{HP}(\vec{r}) + \sum_{\substack{k \geq l \\ k, l \in \text{Types}}} \alpha_{kl} \sum_{\substack{i \in \{\text{Loci of Type } k\} \\ j \in \{\text{Loci of Type } l\}}} f(r_{ij}) + \sum_{d=3}^{500} \gamma(d) \sum_i f(r_{i,i+d})$$

Polymer Potential

Type-Type Interactions

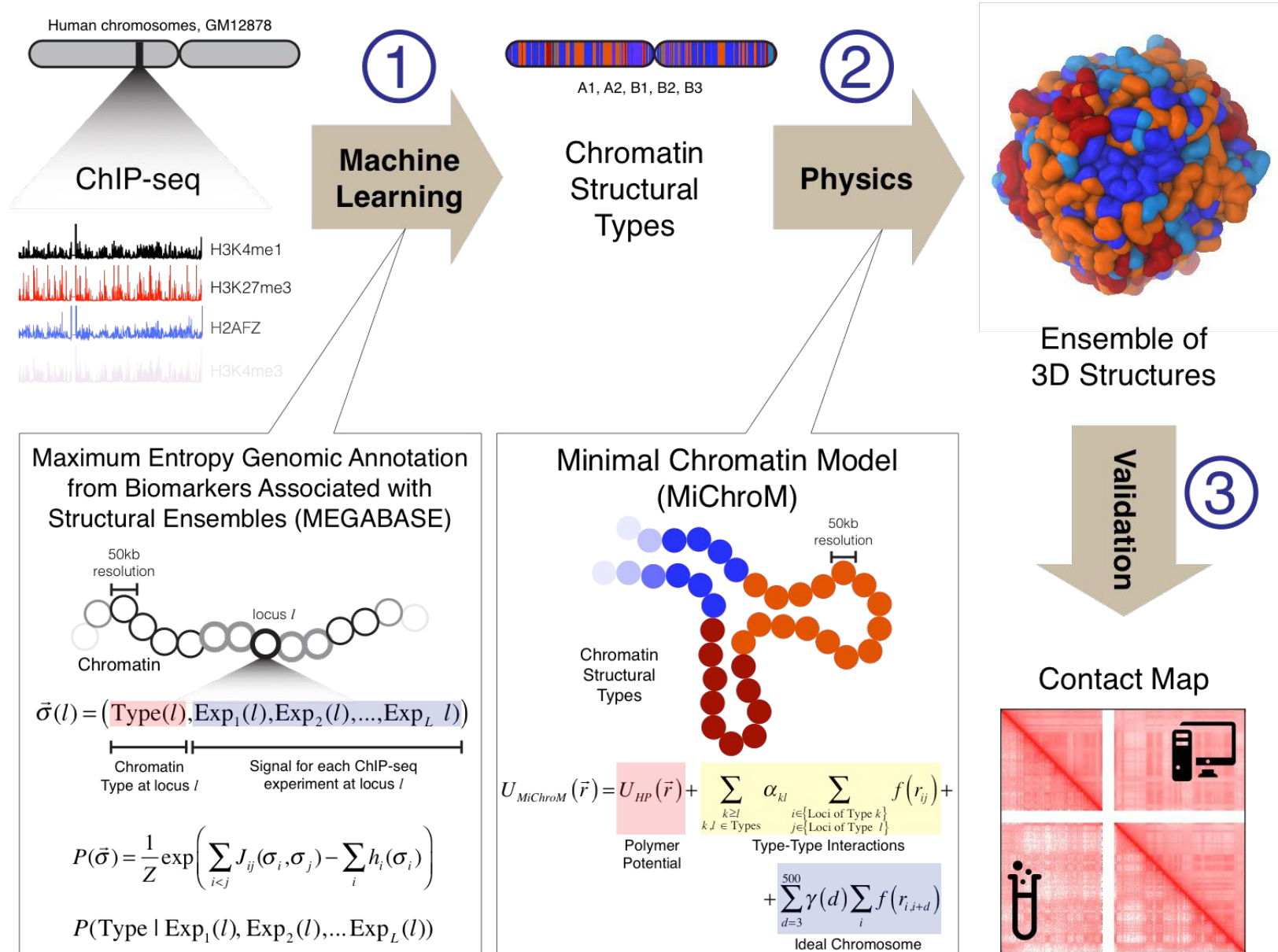
Ideal Chromosome



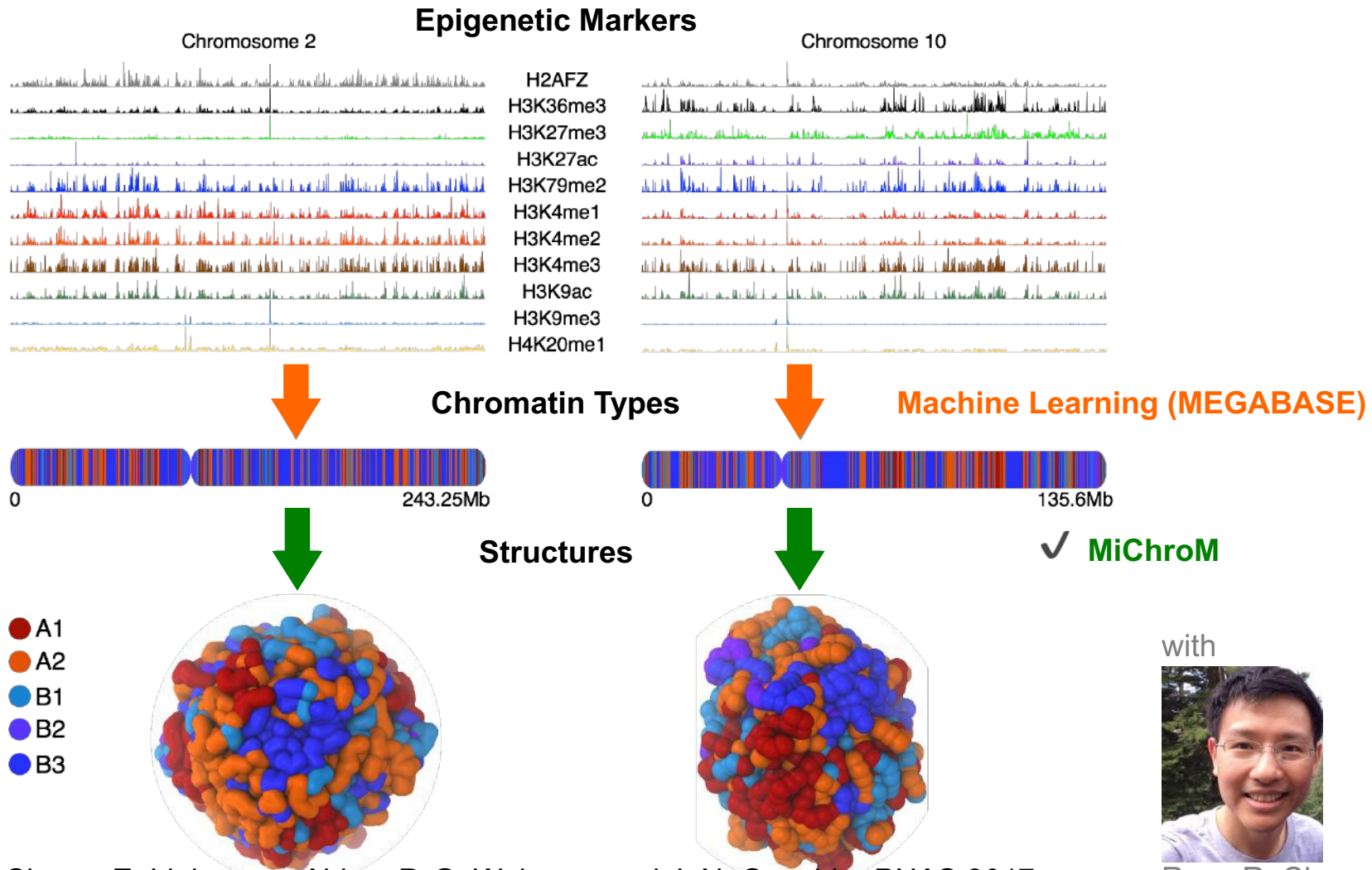
A1, A2, B1, B2, B3, B4

Di Pierro, Zhang, Lieberman Aiden, Wolynes, Onuchic, *PNAS* 2016

Schematic Illustration of Computational Pipeline



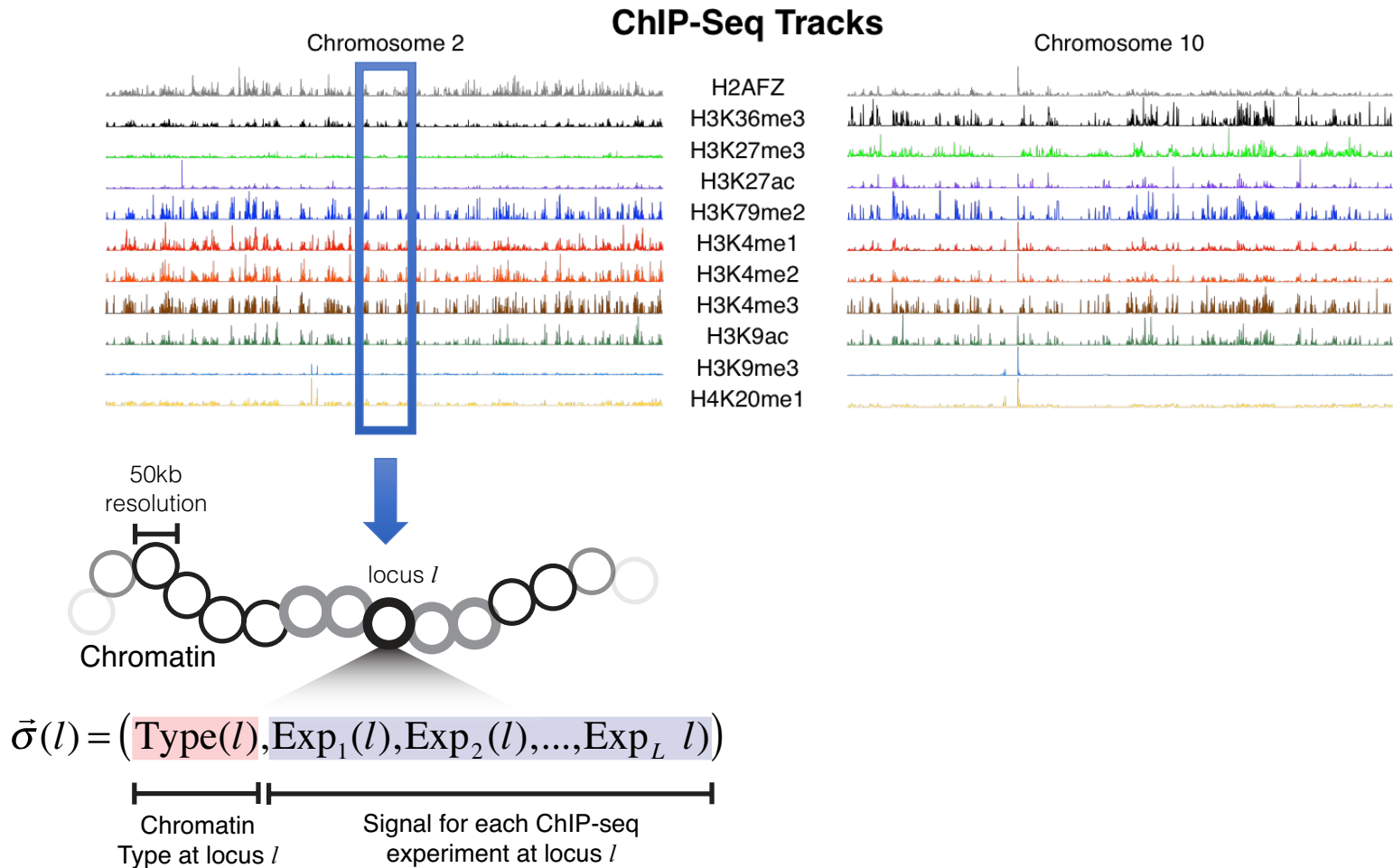
Where Is the Blueprint? From Epigenetics To Chromatin Types (MEGABASE)



M.D.P. , R.R. Cheng, E. Lieberman Aiden, P. G. Wolynes, and J. N. Onuchic, *PNAS* 2017

with
Ryan R. Cheng

De Novo Structure Prediction of Human Chromosomes



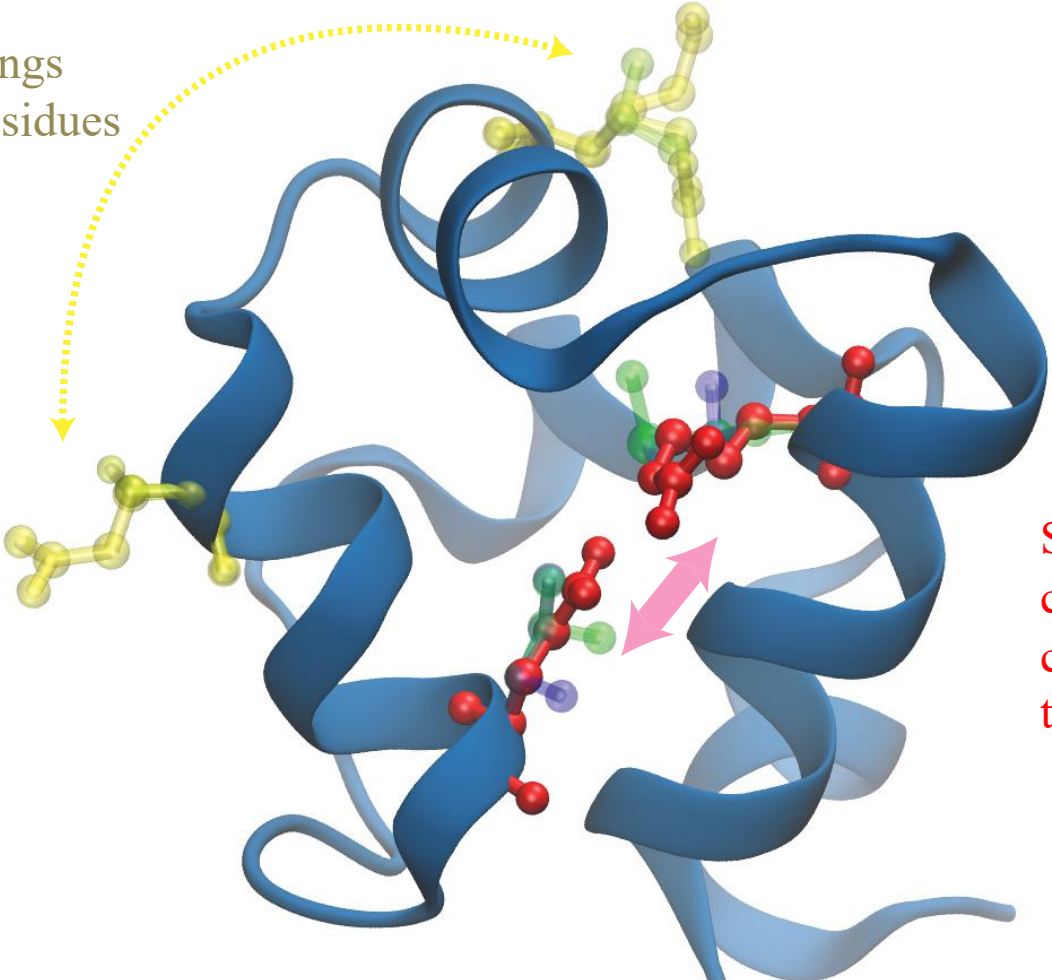
$$P(\vec{\sigma}) = \frac{1}{Z} \exp \left(\sum_{i < j} J_{ij}(\sigma_i, \sigma_j) - \sum_i h_i(\sigma_i) \right)$$

Amino acid coevolution in proteins

Statistical couplings
between distal residues
generally weak

Since 1998

Strong statistical
couplings between
coevolving residues
that are in contact



RPC1_BP434 VKSK**R**IQGLGNQAELAQ**K**VGTT**Q**Q**S**IEQL**E**NGKT-KRPRFLPELASALGVSVDWL
H3Z4N6_STAEP IKS**A**MKEQDMSLSELAR**R**VGVAK**S**AVSRY**L**NLTREFPLNRTEDFAKALSISTEYL
C2X6S5_BACCE IK**K**LLKERALSMRQLG**I**L**T**NI**D**PA**T**VS**R**I**I**NGKQPPKQKHLQKFAECLQVPPQLL



Sequence probability distribution depends on pairwise and single site parameters

```
AAKAP[S]ARGHATKPRAP[K]DAQHEAA
AAKAP[S]ARGHATKPRAP[K]DAQHEAA
SAKEK[N]EKMKIIVKN-L[D]KGGKSGS
TELET[K]FTLDQVKDQLE[E]EQGKKRSS
LAPSG[N]TALATAKKKE[L]TDRTDDPV
TELET[K]FTLDQVKPRAP[K]DGGKRSS
```

$i = 6$

$j = 17$

$$f_{6,17}(S_6, P_{17}) = 2/6$$

Input Data :

$$P_i(A_i) \equiv f_i(A_i)$$

$$P_{ij}(A_i, A_j) \equiv f_{ij}(A_i, A_j)$$

Using maximum entropy principle to model the joint probability distribution

$$C_{ij}(A, B) = f_{ij}(A, B) - f_i(A)f_j(B)$$

$$P(A_1, \dots, A_L) = \frac{1}{Z} \exp\left\{ \sum_{i < j} e_{ij}(A_i, A_j) + \sum_i h_i(A_i) \right\}$$



Faruck Morcos Martin Weight

$$e_{ij}(A, B) \approx -(C^{-1})_{ij}(A, B)$$

Direct Information Metric

Direct Probabilities are defined as:

$$P_{ij}^{(dir)}(A, B) = \frac{1}{Z} \exp\{e_{ij}(A, B) + \hat{h}_i(A) + \hat{h}_i(B)\}$$

The probabilities for residue couplets are ranked using Direct Information

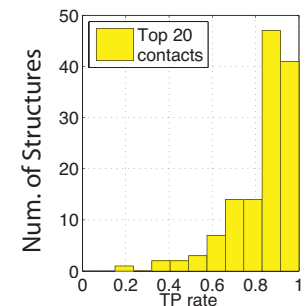
$$DI_{ij} = \sum_{A, B=1}^q P_{ij}^{(dir)}(A, B) \ln \frac{P_{ij}^{(dir)}(A, B)}{f_i(A) f_j(B)}$$

True positive contacts (<8Å) are evaluated from top couplets

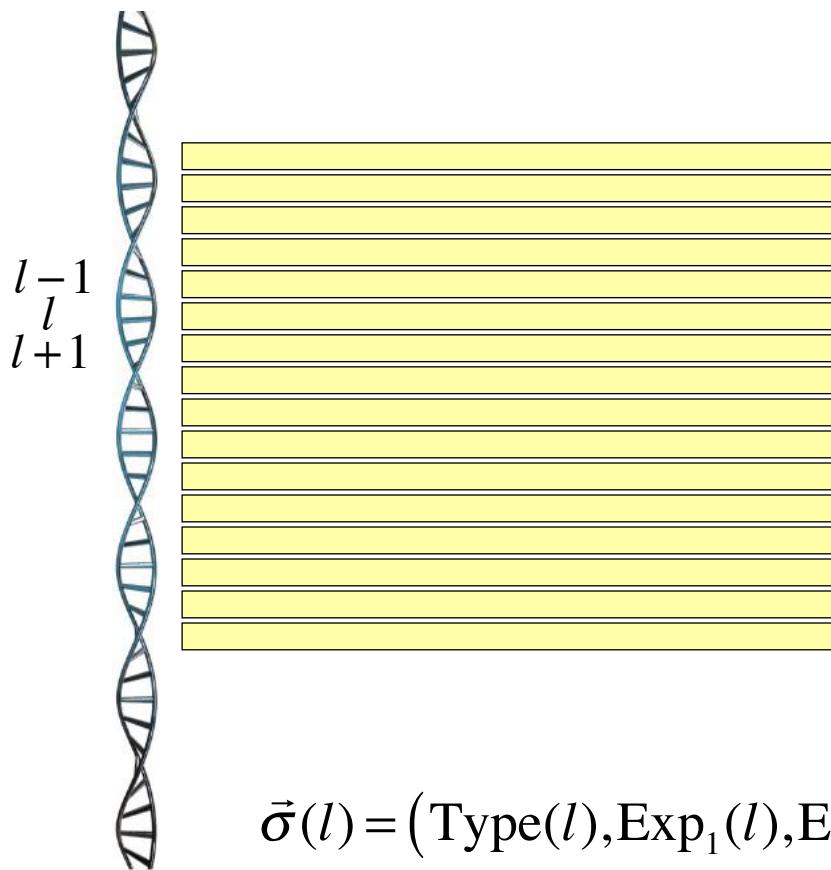
Select top couplets



$|i-j| > 4$



True Positive (TP) rates

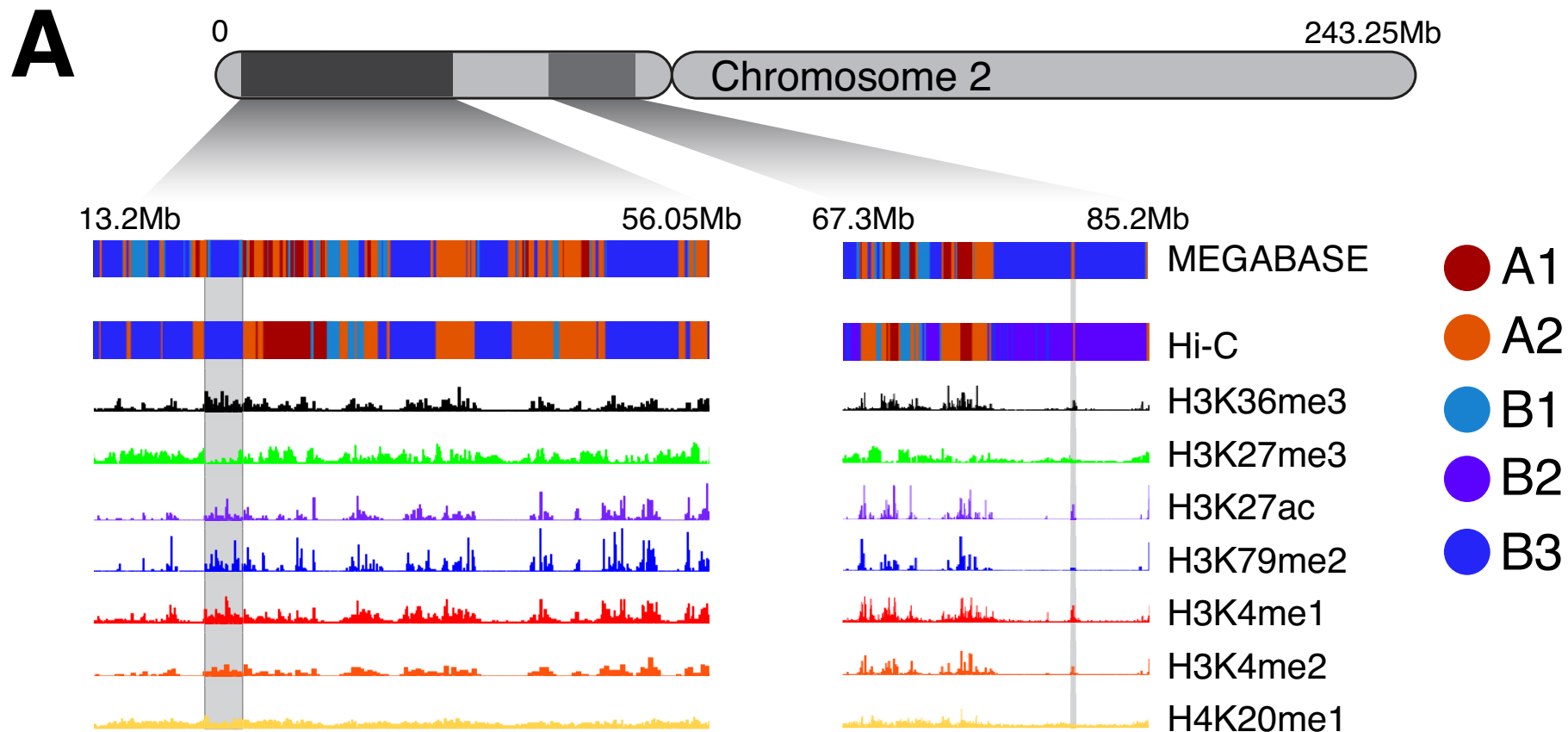


$$P(\vec{\sigma}) = \frac{1}{Z} \exp(-H(\vec{\sigma}))$$

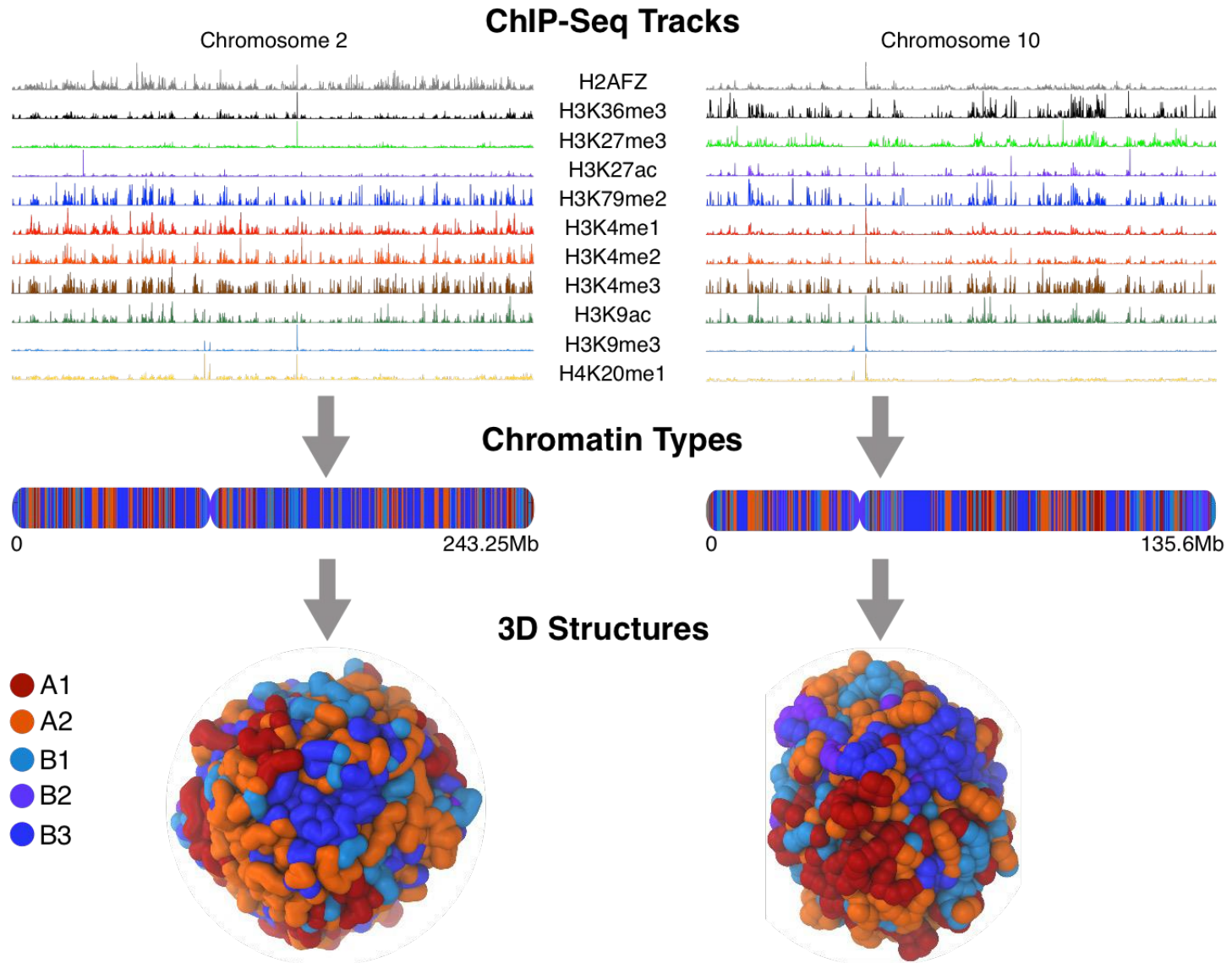
$$H(\vec{\sigma}) = -\sum_{i < j} J_{ij}(\sigma_i, \sigma_j) - \sum_i h_i(\sigma_i)$$

Training set: odd-numbered chromosomes

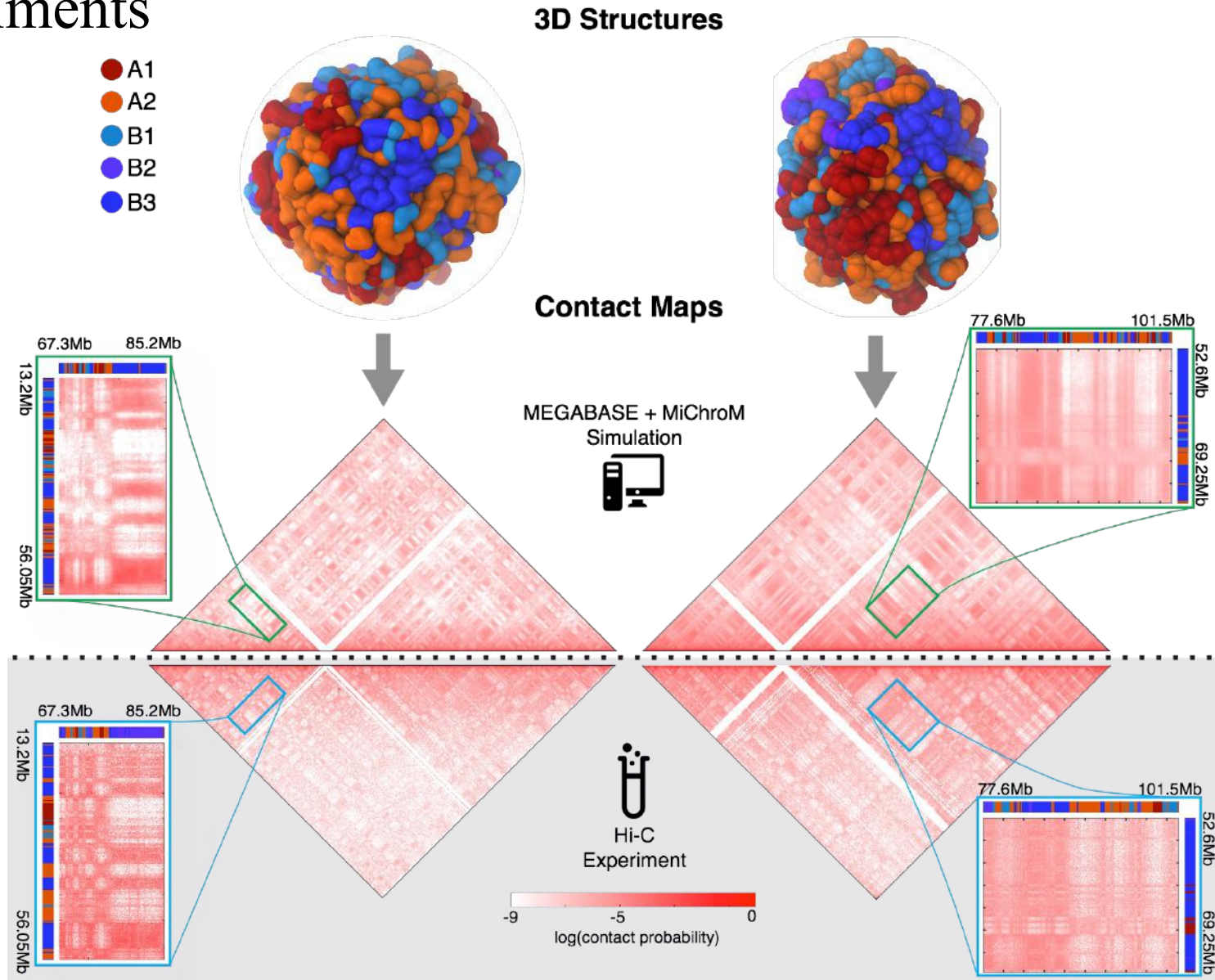
Test set: even-numbered chromosomes



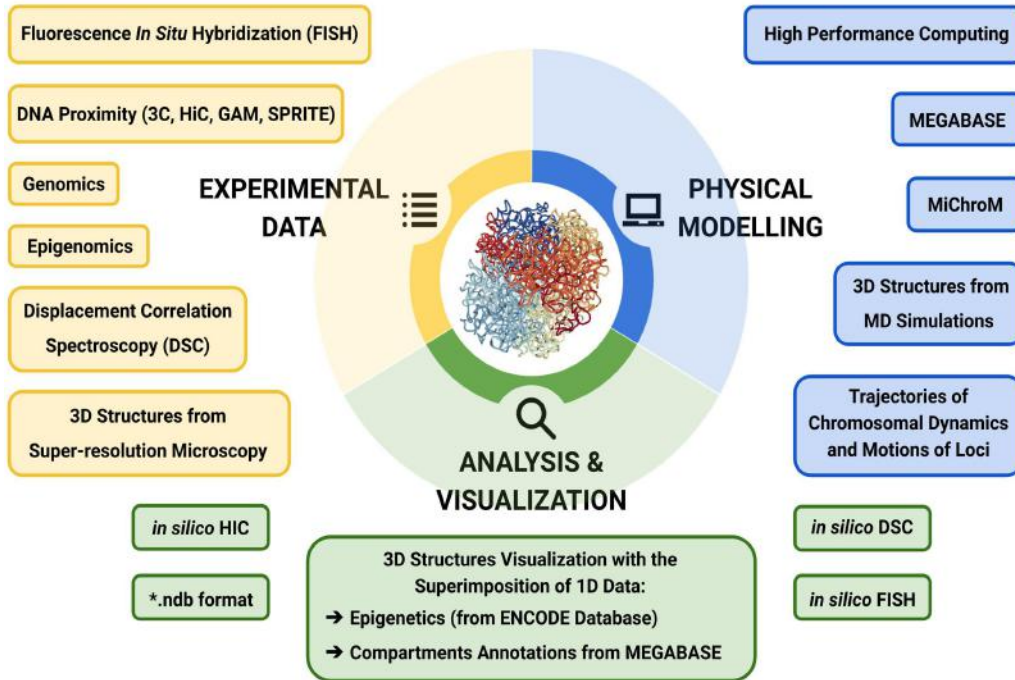
De Novo Structure Prediction of Human Chromosomes



Comparison of simulated structures with DNA-DNA Ligation Experiments



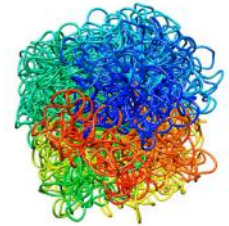
The Nucleome Data Bank



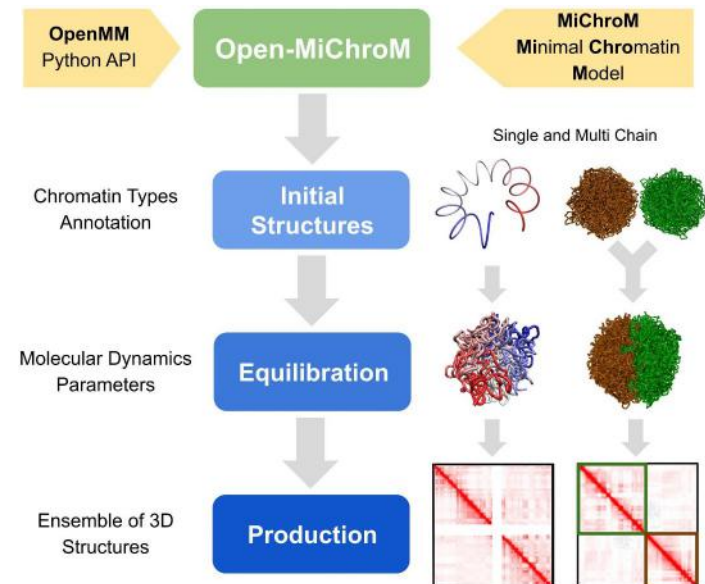
Nucleosome Data Bank

A web platform to simulate and browse the three-dimensional architecture of genomes

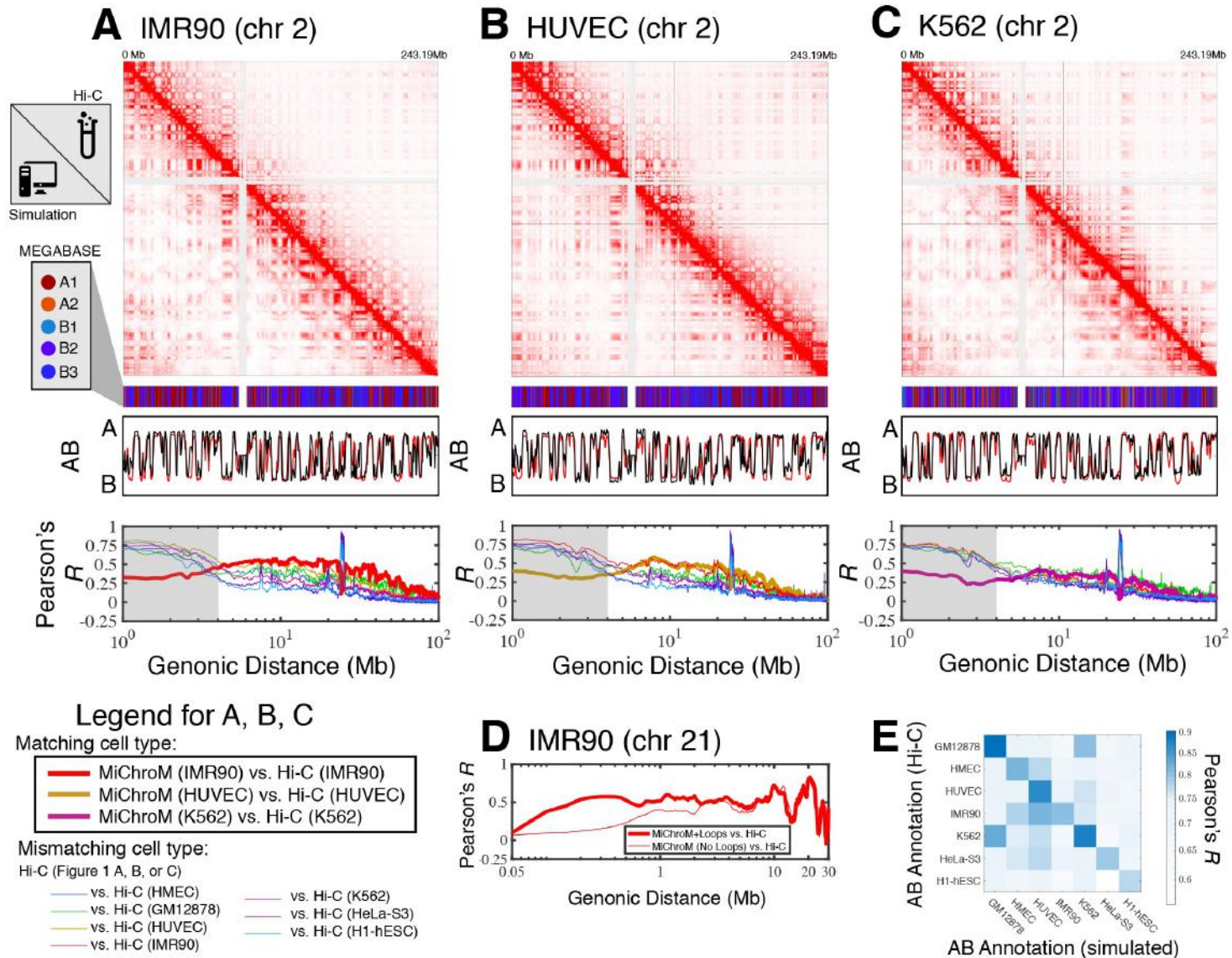
3D ensemble of Chromosomal Structures



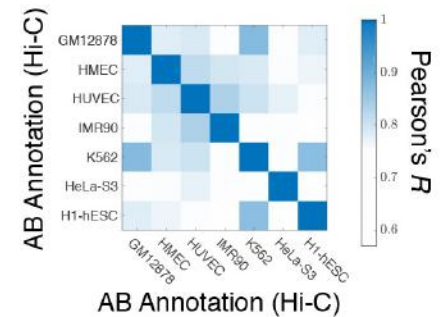
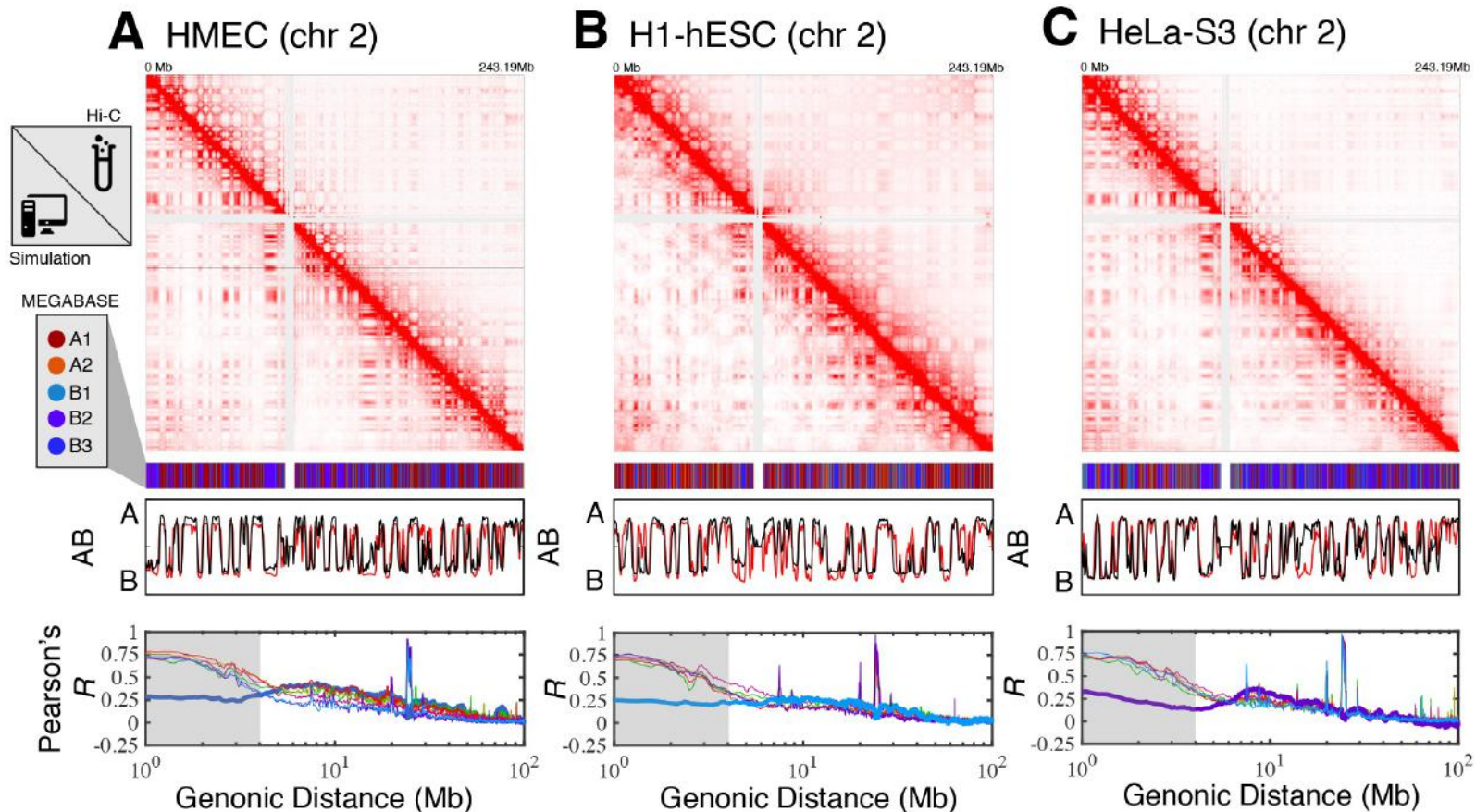
Open-MiChroM



Prediction of chromosome structures for differentiated cell lines and for immortalized leukemia cells.

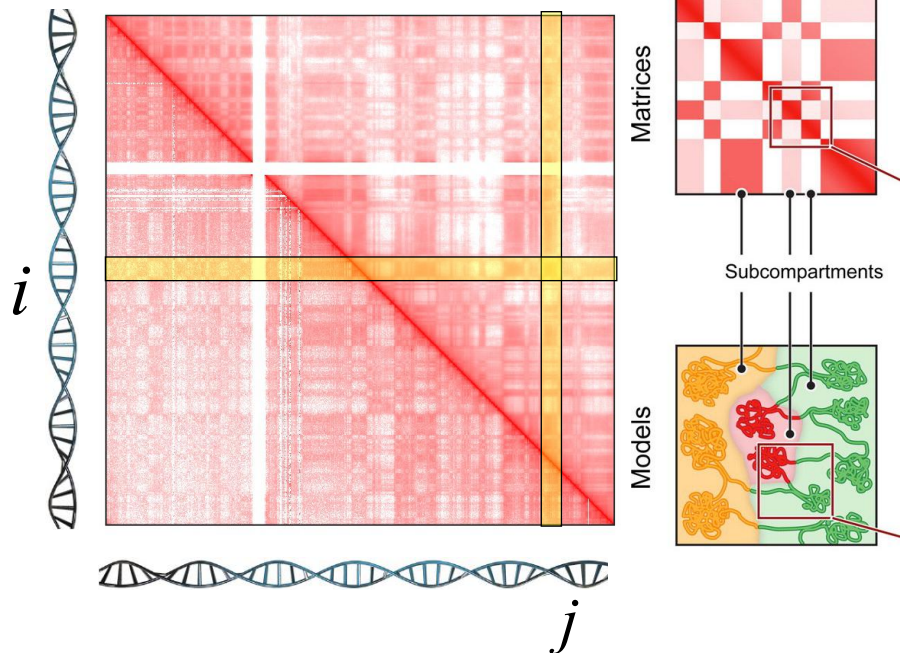


Prediction of chromosome structures for HMEC, H1-hESC, and HeLa-S3.



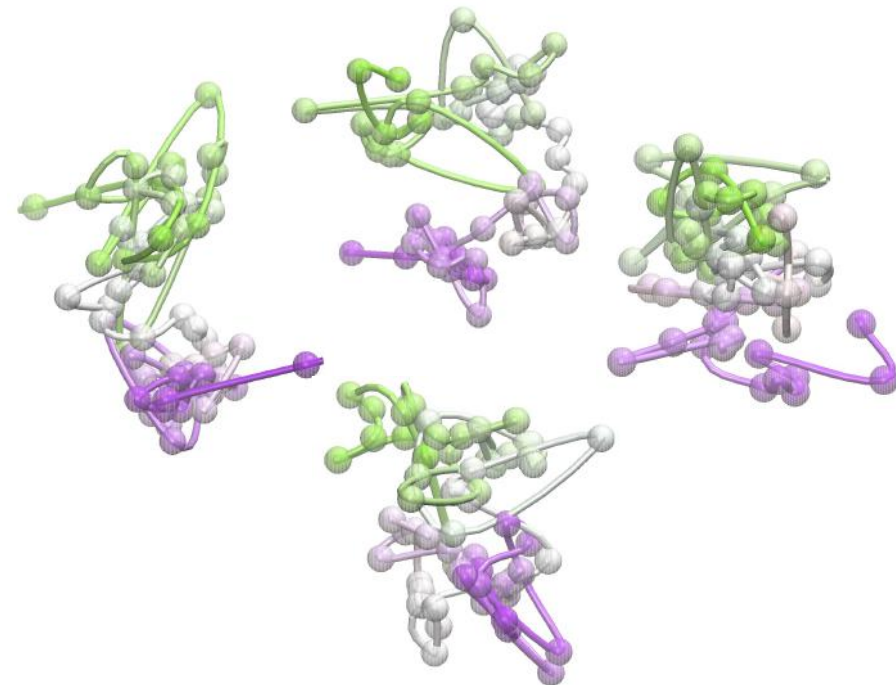
Chromosome Structural Heterogeneity: No two structures are identical

DNA-DNA ligation map
(population averaged)



Rao & Huntley et al, Cell 2014

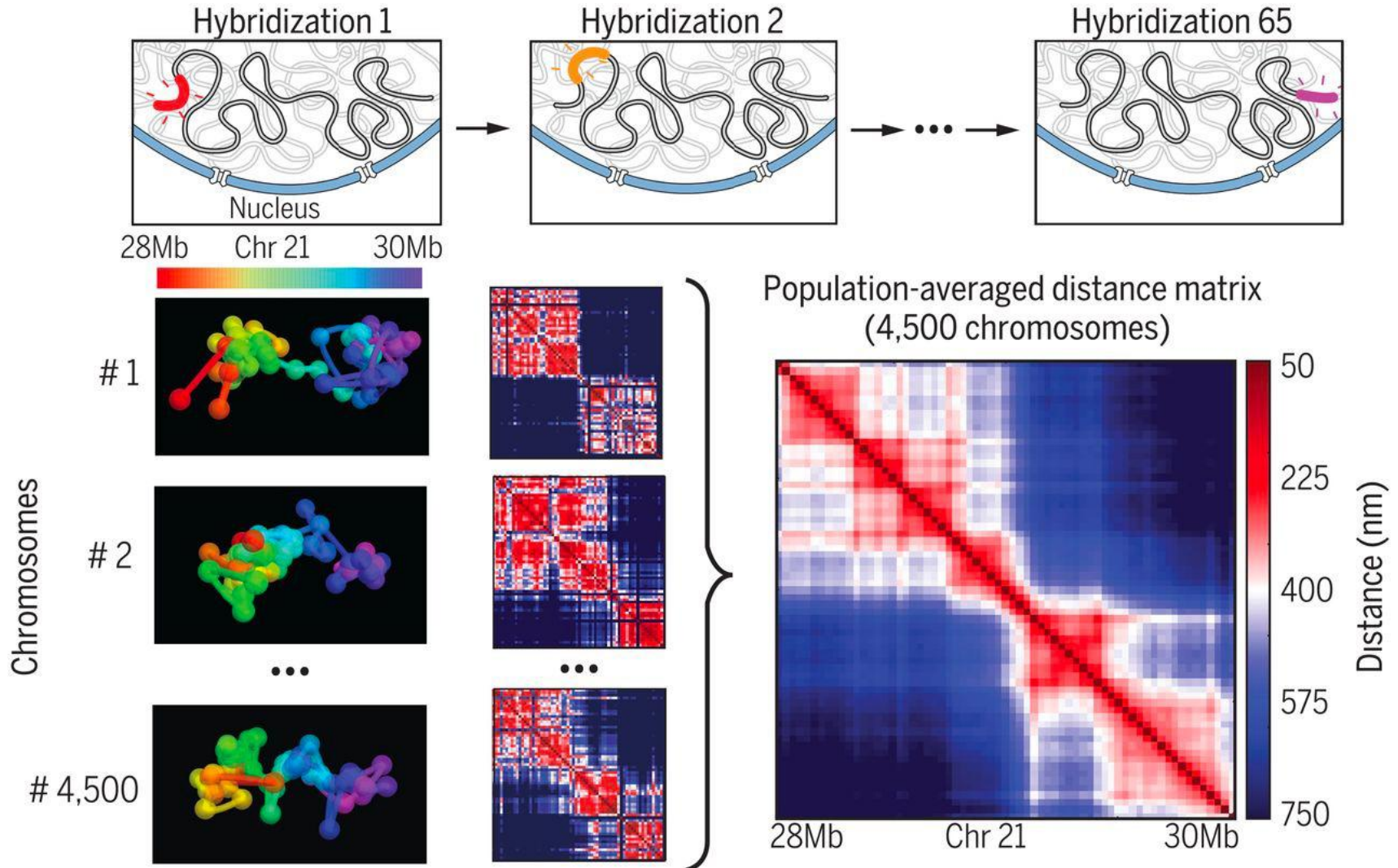
3D structures of chromatin
(DNA tracing/microscopy)



Bintu et al, Science 2018

Super-resolution imaging of chromatin

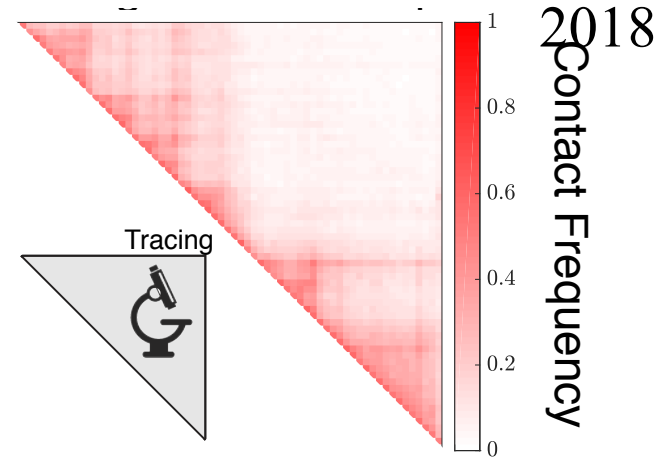
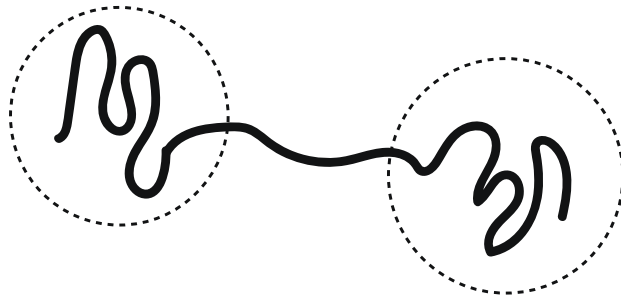
B. Bintu and L. Mateo..... A. Boettiger, Xiaowei Zhuang, *Science*



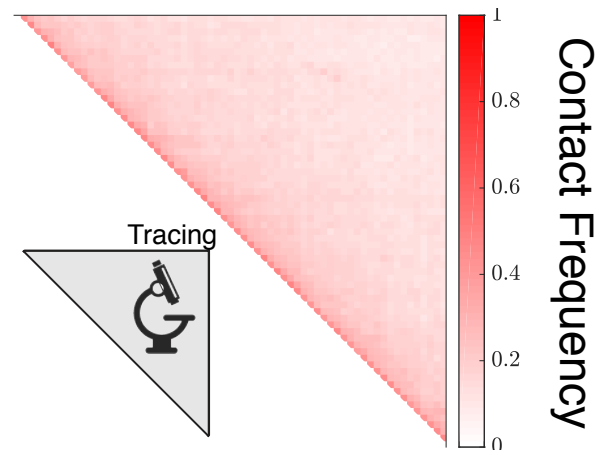
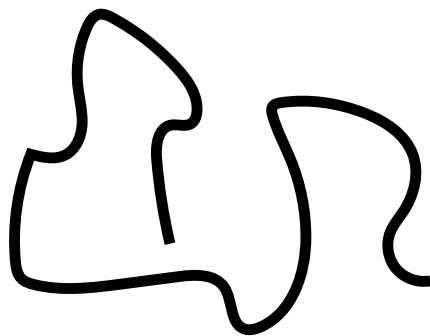
Super-resolution imaging of chromatin

B. Bintu and L. Mateo..... A. Boettiger, Xiaowei Zhuang, *Science*

Loop domains form globular lobes at the head and tail of Segment 1



Segment 1: chr21 29.37-31.32 Mb

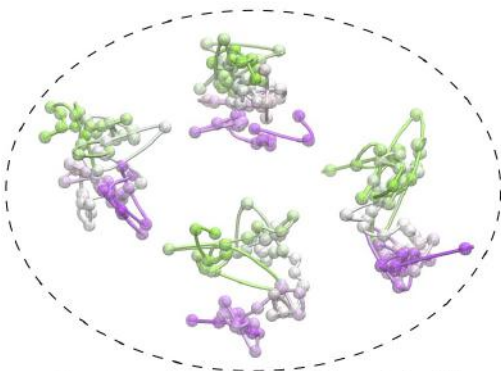


Segment 2: chr21 20.0-21.9 Mb

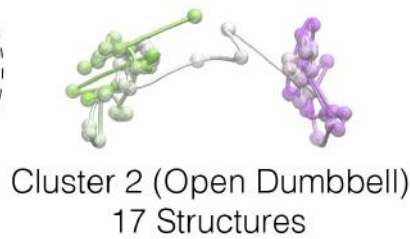
ANALYSIS OF CHROMATIN STRUCTURES REVEAL STRUCTURAL TRANSITIONS: OPEN VS. CLOSED

Experimentally Traced Structures (Bintu et al *Science* 2018)
IMR90 chromosome 21: 29.37-31.32Mb

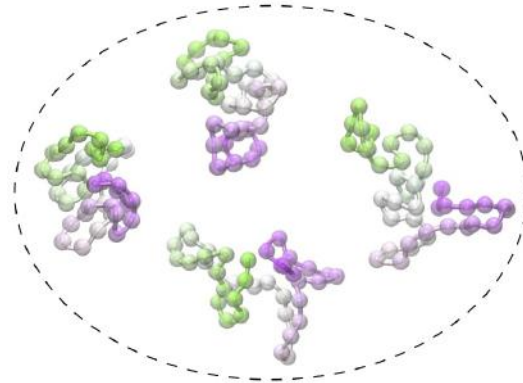
Simulated Structures (MiChroM)
IMR90 chromosome 21: 29.37-31.32Mb



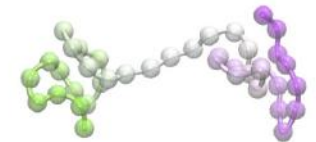
Cluster 1 (Closed Dumbbell)
912 Structures



Cluster 2 (Open Dumbbell)
17 Structures



Cluster 1 (Closed Dumbbell)
6275 Structures



Cluster 2 (Open Dumbbell)
125 Structures

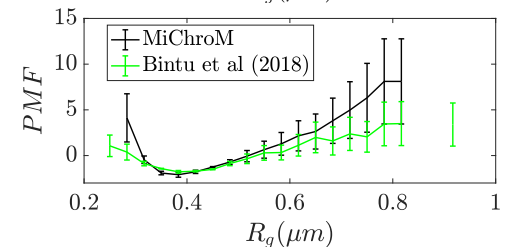
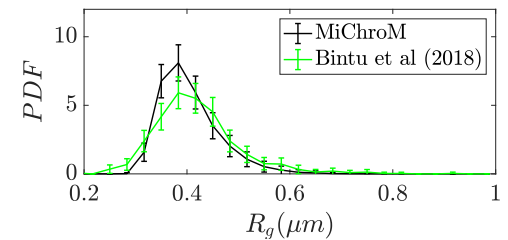
Structural similarity order parameter:

$$Q_{AB} = \frac{1}{N} \sum_{i,j} \exp\left(-\frac{(r_{ij}^A - r_{ij}^B)^2}{2\delta^2}\right)$$

$$\delta = 0.165 \mu\text{m}$$

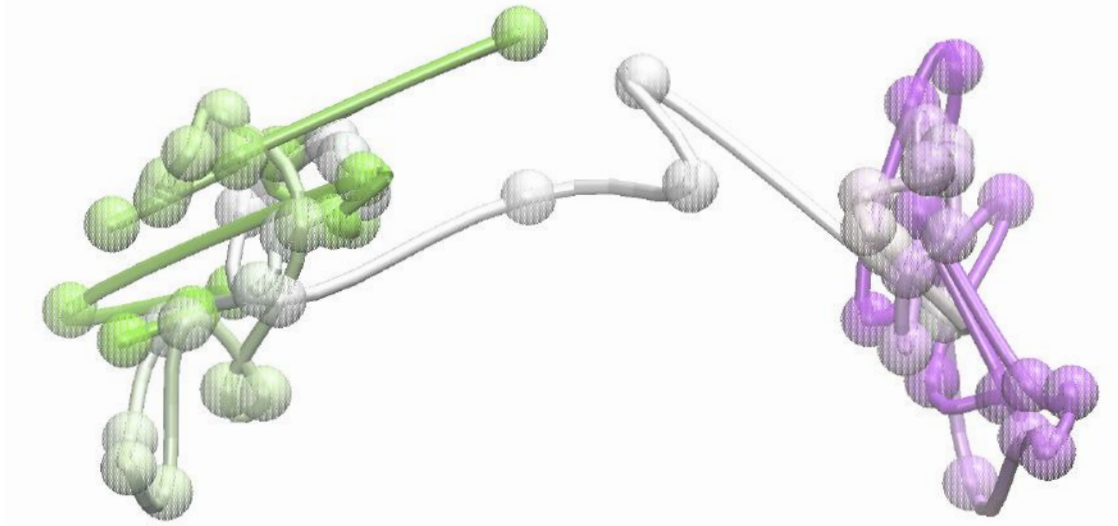
Free energy difference between open and closed structures (experiment & simulation):

$$\log(N_{\text{closed}} / N_{\text{open}}) = E_{\text{open}} - E_{\text{closed}} \sim 4k_B T$$



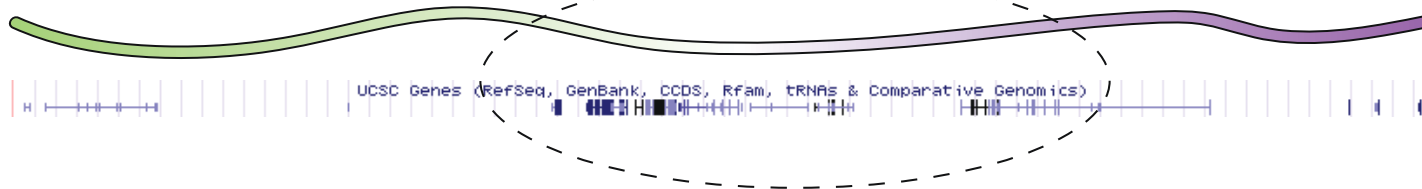
A relationship between gene expression and chromosome structure?

Genes primarily located in linker region



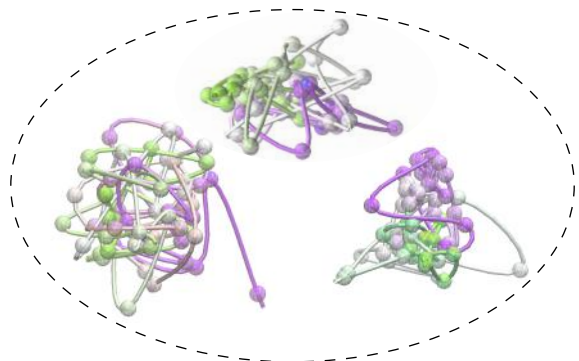
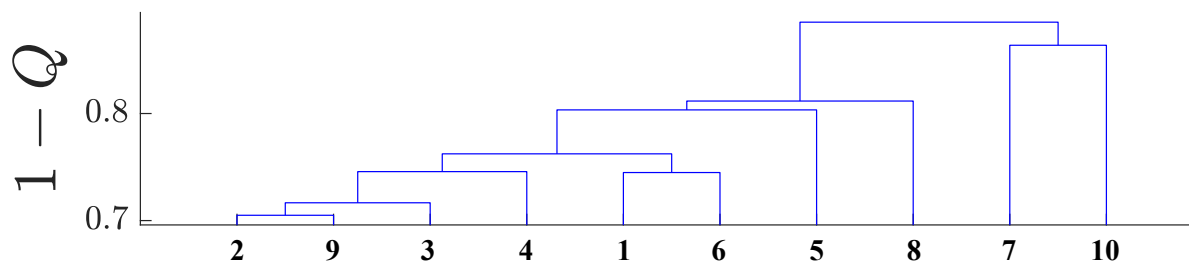
29.37Mb

31.32Mb

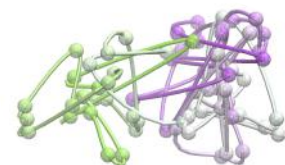


Analysis of Experimental Traced Chromatin Structures of Segment 2

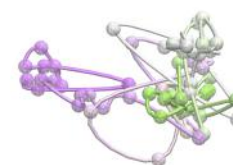
A Hierarchical Clustering of Traced Structures of IMR90 Segment 2 (chr21 20.0-21.9 Mb)



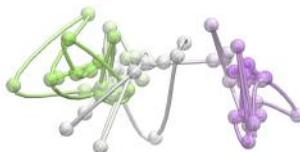
Cluster 1 (711 structures)



Cluster 6 (13 structures)



Cluster 3 (11 structures)

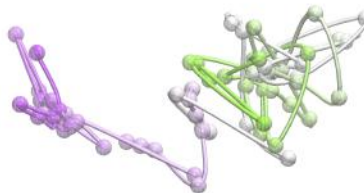


Cluster 5 (8 structures)



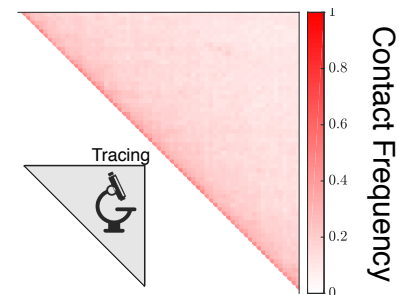
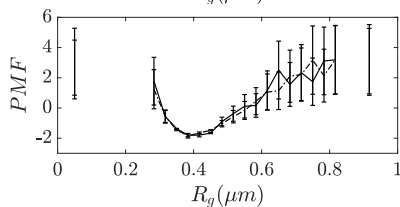
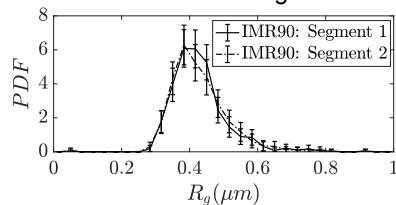
Cluster 8 (2 structures)

Artifact



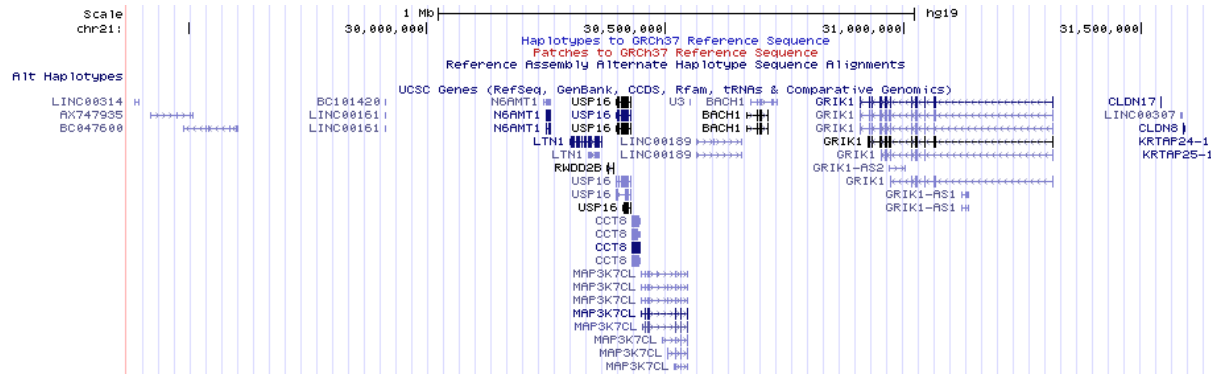
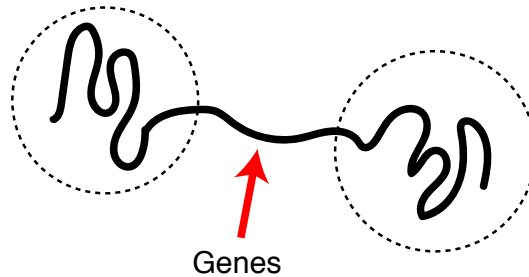
Cluster 7 (3 structures)

B Distribution of R_g and Potential of Mean Force for Segment 1

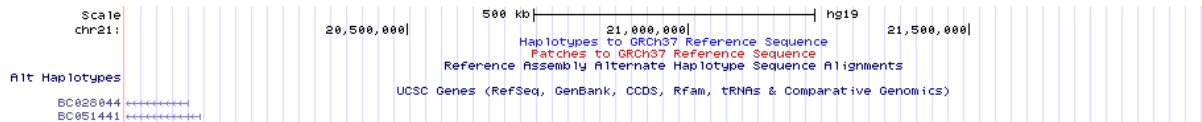
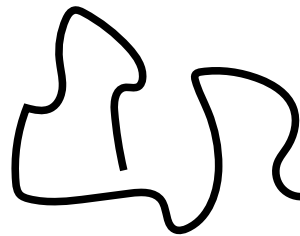


A relationship between gene expression and chromosome structure?

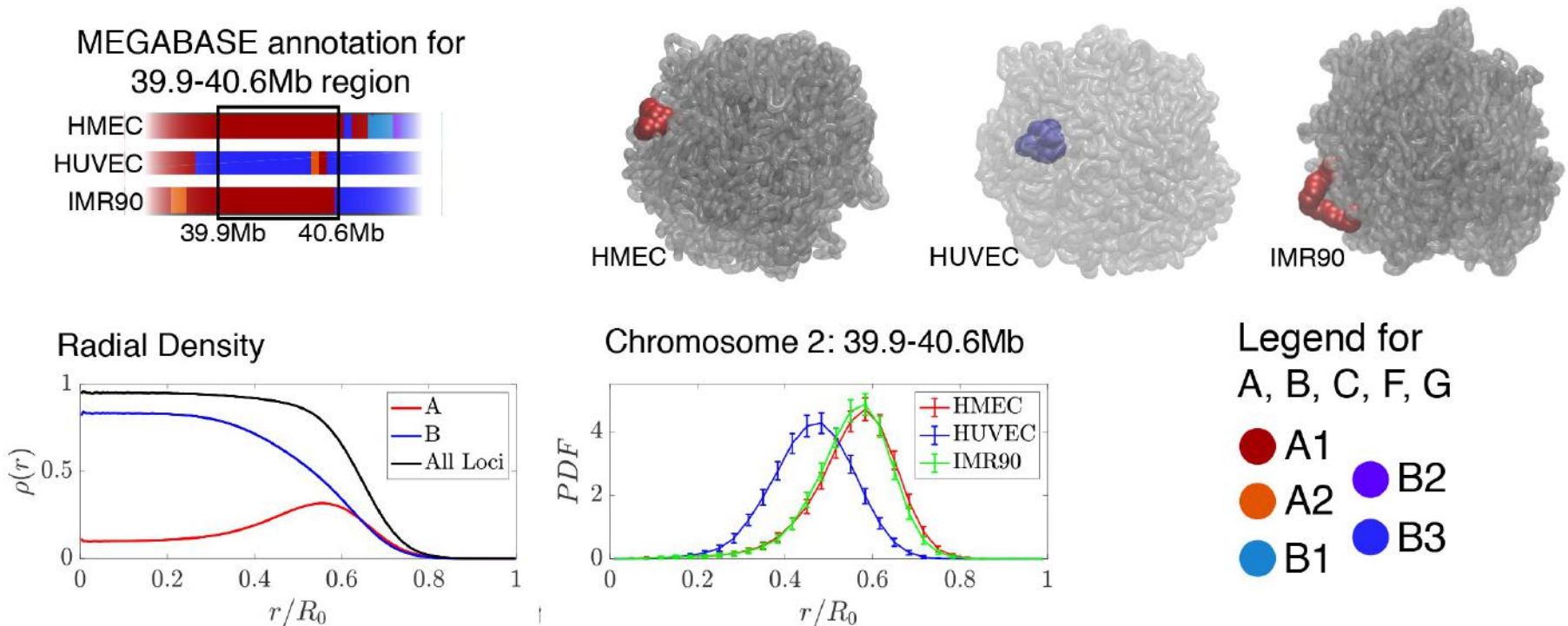
A Segment 1 (29.37-31.32Mb)
 Loop domains form globular lobes at the head and tail of Segment 1



B Segment 2 (20.0-21.9Mb)
 No CTCF-mediated loops
 Random coil-like structures

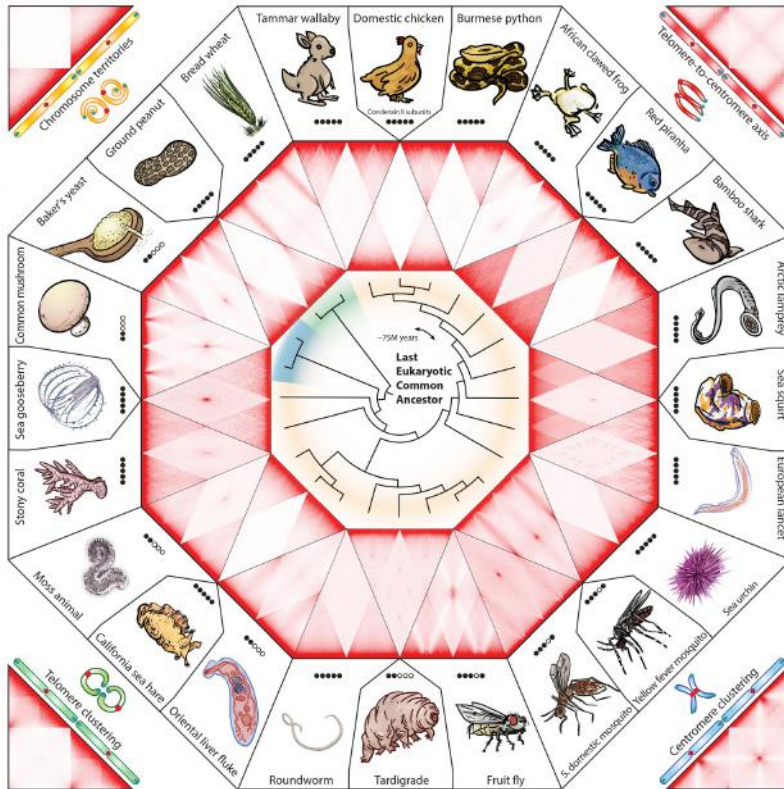


A-compartment chromatin moves to territorial surface



Consistent with experimental observations: Nagano, T., et al., Single-cell Hi-C reveals cell-to-cell variability in chromosome structure. Nature, 2013. 502(7469): p. 59-64.

CHROMOSOME ARCHITECTURE ACROSS EVOLUTION CORRELATES WITH CONDENSIN II ACTIVITY

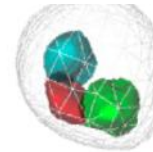
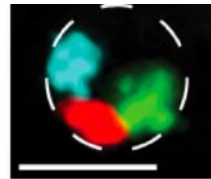


Hoencamp et al., *Science* (2021)

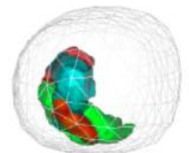
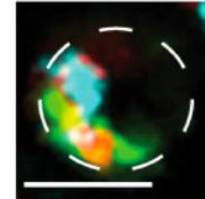
Type I architecture	Type II architecture
Centromere clustering ➤	Chromosome territories ➤
Telomere clustering ➤	All condensin II subunits present ➤
Telo-to-centromere axis ➤	
One or more condensin II subunits absent ➤	

Condensin II (loop-extruding enzyme) confers longitudinal rigidity to chromosomes and defines **chromosome territories** (Houlard et al., *Nat. Cell Biol.* 2015, Bauer et al. *PLoS Genet.* 2012; Rosin et al. *PLoS Genet.* 2018, ...)

Wild Type

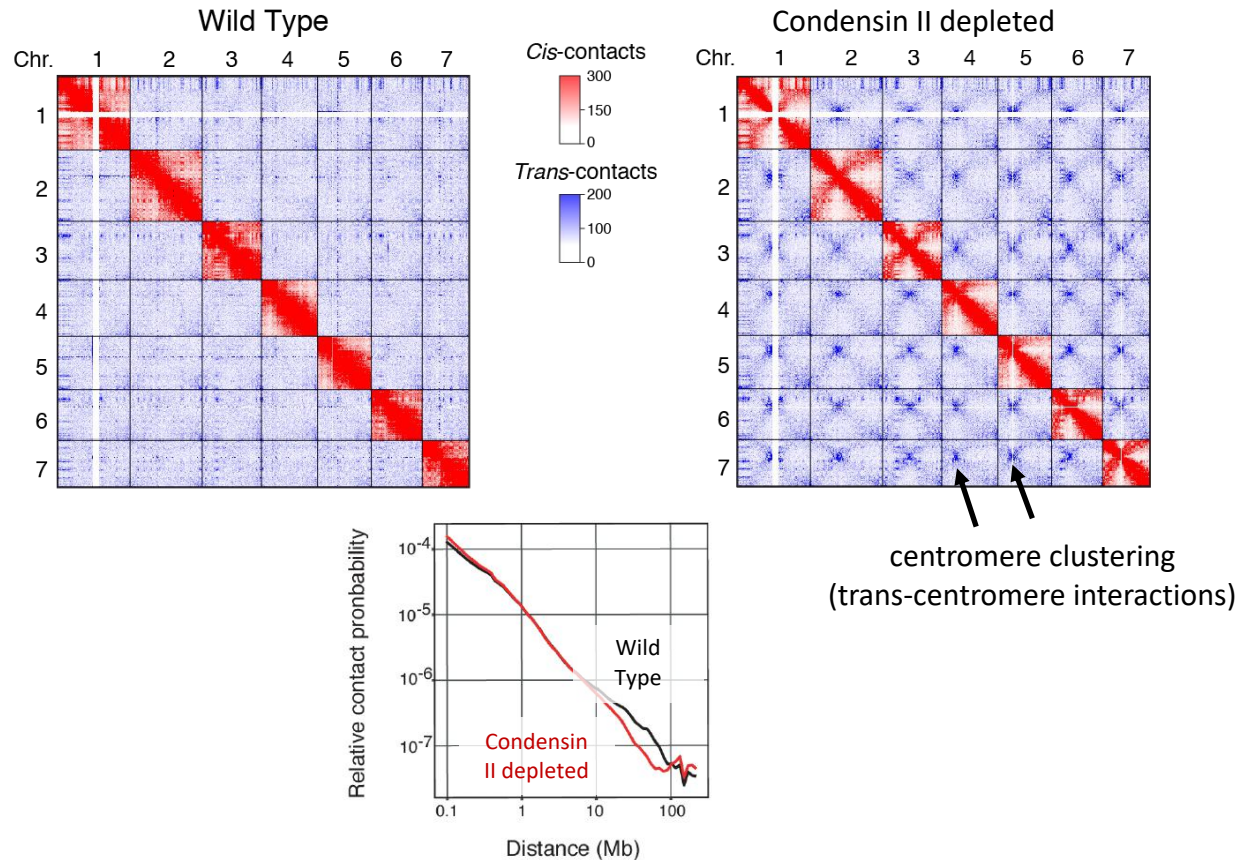
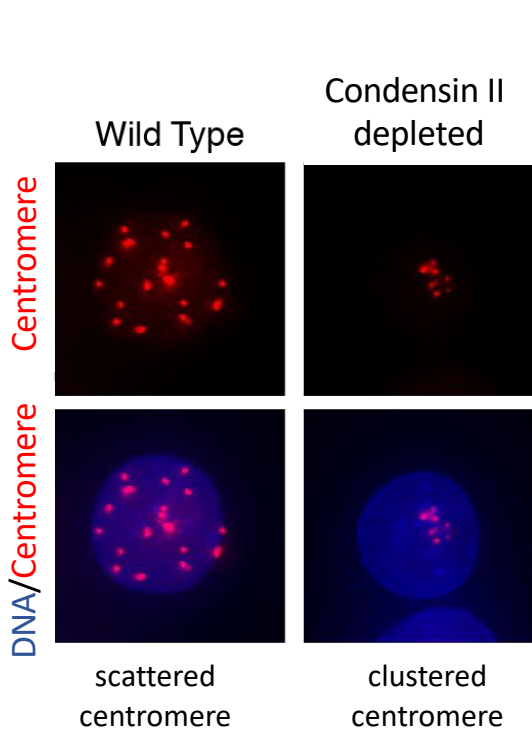


Condensin II depletion



Rosin et al. *PLoS Genet.* 2018

CONDENSIN II DEPLETION LEADS TO A PHENOTYPE WITH CLUSTERED-CENTROMERES AND LOWER CIS-COMPACTION



Hoencamp et al., *Science* (2021)

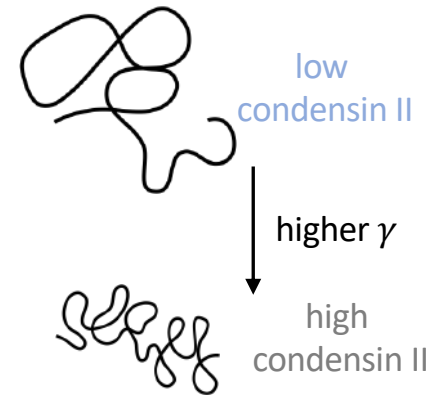
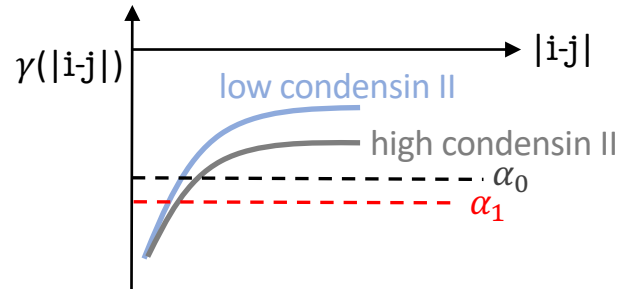
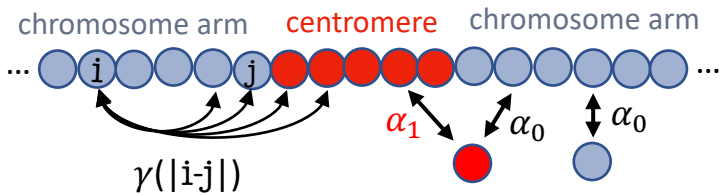
MICROM INTERACTIONS AND LENGTHWISE COMPACTION ACTIVITY OF CONDENSIN II

$$U_{MiChroM}(\vec{r}) = U_{HP}(\vec{r}) + \sum_{\substack{k \geq l \\ k, l \in \text{Types}}} \alpha_{kl} \sum_{\substack{i \in \{\text{Loci of Type } k\} \\ j \in \{\text{Loci of Type } l\}}} f(r_{ij}) + \chi \sum_{(i,j) \in \{\text{Loop Sites}\}} f(r_{ij}) + \sum_{d=3}^{d_{cutoff}} \gamma(d) \sum_i f(r_{i,i+d})$$

Homopolymer Flory-like two-body term CTCF loops Ideal Chromosome

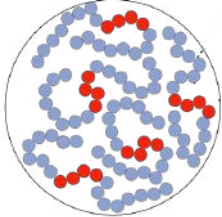
Polymer connectivity
Topology fluctuations Phase separation of
Heterochromatin (centromeres) Lengthwise compaction
Loop extrusion activity
(condensin II)

Simplified model (competition between phase separation and lengthwise compaction):



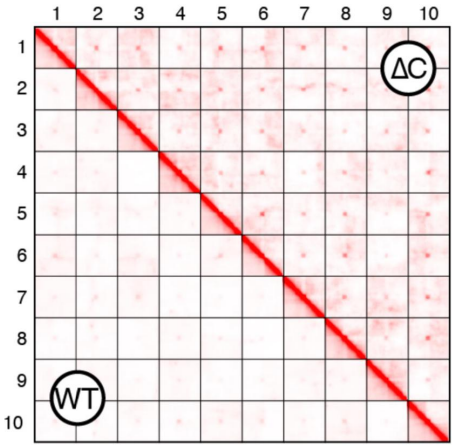
CONDENSIN II ACTIVITY (LENGTHWISE COMPACTION) COUNTERACTS CENTROMERE CLUSTERING

genome with multiple chromosomes



WT : condensin II active (high γ)

ΔC : condensin II inactive (low γ)



WT : condensin II active (high γ)

strong chromosome territories

scattered centromeres (red)

centromere (red) buried in a chromosome territory (cyan)

ΔC : condensin II inactive (low γ)

weak chromosome territories

clustered centromeres (red)

centromere (red) exposed due to weak chromosome territory (cyan)

Hoencamp et al., *Science* (2021)

Postdocs:

Ryan Cheng, Sumithaba Brahmachari, Vinicius Contessoto,
Antonio Oliveira Jr.,
Dongya Jia - NIH
Susmita Roy – IISER – India
Fang Bai – Shanghai Tech, China * Michele Di Piero NorthEastern
Ellinor Haglund – Hawaii * Heiko Lammert - Karlsruher
Faruck Morcos, - Univerisity of Texas at Dallas
Mingyang Lu – Northeastern * Jeff Noel - Max Delbruck Center, Berlin
Alex Schug - Karlsruher Institut für Technologie (KIT)
Biman Jana – Indian Assoc. Cultivation of Science - India
Joanna Sulkowska – University of Warsaw
Koby Levy - Weizmann Institute * Changbong Hyeon - KIAS, Korea
Cecilia Clementi – Rice University * Joan-Emma Shea – UCSB
Adelia Aquino – Texas Tech * Steve Plotkin – UBC, Canada
Osamu Miyashita – RIKEN, Japan
John Finke - University of Washington, Tacoma
Antitsa Stoycheva - Gilead Sciences, Inc.
Nick Socci – Sloan Katering
Yoko Suzuki - Meisei University – Tokyo
Chigusa Kobayashi - RIKEN, Japan
Eric Nelson – UTSWMC, Texas
Jian Liu - NIH
Shachi Gosavi - NCBS – India
Dana Krepel – Biotech Israel
Daniel Schultz – Harvard
Leandro Oliveira and Jorge Chahine - UNESP, Brazil
Marcio de Mello Cardoso – UFRJ, Brasil

Students

Kareen Mehrabiani, Weiqi Lu, Madelin Galbraith, Esteban Rojas, Erdong Ding, Mattheus Mello, Ragini Mahajan
Federico Bocci – UC Iirvine
Xingcheng Lin – MIT
Bin Huang – private company
Nathan Eddy - Indigo
Lis Sun - China
Marcelo Boareto – ETH Zurich, Switzerland
Ricardo Santos – University of Campinas, Brazil
Ryan Heyes – University of Michigan
Mohit Raghunathan – Amazon Seattle
Paul Whitford – Northeastern University
Hugh Nymeyer – Florida State University
Marcos Betancourt – BMCC New York
Vitor Leite - UNESP, Brazil
Leslie Chavez - LANL
Margaret Cheung - University of Houston
Sichun Yang – Case Western University
Peter Leopold – BioAnalyte Inc.

Collaborators

Peter Wolynes, Herbie Levine, Erez Lieberman Aiden
Ben Rowland - Netherlands Cancer Institute
Jianpeng Ma – Baylor College of Medicine
Angel Garcia and Karissa Sanbonmatsu - LANL
Pat Jennings and Terry Hwa– UCSD
Martin Weigt – Univ. Paris, France
Samuel Flores – Univ. of Uppsala, Sweden
Zan Luthey-Schulten – UIUC
Glaucius Oliva and Adriano Andricopulo - USP, Brazil
Hualiang Jiang – SIMM Chins
Charles Brooks – U. Michigan
Stefan Klumpp – MPIKG, Germany
Shoji Takada - Kobe, Japan
Ashok Deniz – TSRI
Mikael Oliverberg – Stockholm
Antonio Francisco Pereira de Araujo – Brasilia
Yoshitaka Tanimura - Kyoto, Japan
Yuko Okamoto – Nagoya University, Japan
Ulrich Hansmann – University of Arkansas
Rachel Nechushtai – Hebrew University
Ron Mittler – Univ. North Texas
Jeff Tabor – Rice Univ.



National Science Foundation
WHERE DISCOVERIES BEGIN

